COMBUSTION GAS GENERATOR FOR GAS TURBINE EXHAUST SYSTEMS MODELING

Paul Davidson Ross

Report Number: NPS69-77-0005

NAVAL POSTGRADUATE SCHOOL
Monterey, California

THESIS

COMBUSTION GAS GENERATOR FOR
GAS TURBINE EXHAUST SYSTEMS
MODELING
by

Paul Davidson Ross, Jr.

December 1977

Thesis Advisor: Paul F. Pucci

Prepared for: Naval Sea Systems Command
Washington, D.C.
Code 0331

SECURITY CLASSIFICATION OF THIS PAGE (When Data Entered)

REPORT DOCUMENTATION PAGE

READ INSTRUCTIONS BEFORE COMPLETING FORM

1. REPORT NUMBER: NPS69-77-0005	2. GOVT ACCESSION NO.
3. RECIPIENT'S CATALOG NUMBER	
4. TITLE (and Subtitle): Combustion Gas Generator for Gas Turbine Exhaust Systems Modeling	5. TYPE OF REPORT & PERIOD COVERED: Thesis Report, FY78
6. PERFORMING ORG. REPORT NUMBER	
7. AUTHOR(s): Paul Davidson Ross, Jr.	8. CONTRACT OR GRANT NUMBER(s)
9. PERFORMING ORGANIZATION NAME AND ADDRESS: Naval Postgraduate School, Monterey, California 93940	10. PROGRAM ELEMENT, PROJECT, TASK AREA & WORK UNIT NUMBERS: N0002477WR76119
11. CONTROLLING OFFICE NAME AND ADDRESS: Naval Postgraduate School, Monterey, California 93940	12. REPORT DATE: December 1977
	13. NUMBER OF PAGES: 110
14. MONITORING AGENCY NAME & ADDRESS (if different from Controlling Office)	15. SECURITY CLASS. (of this report): Unclassified
	15a. DECLASSIFICATION/DOWNGRADING SCHEDULE

16. DISTRIBUTION STATEMENT (of this Report)

Approved for public release; distribution unlimited.

17. DISTRIBUTION STATEMENT (of the abstract entered in Block 20, if different from Report)

18. SUPPLEMENTARY NOTES

19. KEY WORDS (Continue on reverse side if necessary and identify by block number)

Gas Generator
Exhaust Gas Eductors
Gas Turbine Exhaust Model

20. ABSTRACT (Continue on reverse side if necessary and identify by block number)

A combustion gas generator was constructed for the purpose of modeling shipboard gas turbine engine exhaust systems. In particular, the system was designed and validated for exhaust stack temperatures varying from 700 to 900°F with an exhaust stack inside diameter of

(20. ABSTRACT Continued)

7.122 inches. Additionally a proposed gas turbine exhaust four-nozzle eductor system was constructed for testing under high temperature conditions to verify temperature correlation parameters developed using cool air as the primary flow medium. A secondary air flow metering box was designed and partially completed for the determination of eductor pumping characteristics during hot flow operations.

Approved for public release; distribution unlimited.

Combustion Gas Generator for Gas Turbine Exhaust Systems Modeling

by

Paul Davidson Ross, Jr.
Lieutenant Commander, United States Navy
B.S., Princeton University, 1966

Submitted in partial fulfillment of the
requirements for the degree of

MASTER OF SCIENCE IN MECHANICAL ENGINEERING

from the

NAVAL POSTGRADUATE SCHOOL
December 1977

ABSTRACT

A combustion gas generator was constructed for the purpose of modeling shipboard gas turbine engine exhaust systems. In particular, the system was designed and validated for exhaust stack Mach numbers in the neighborhood of 0.07 and exhaust stack temperatures varying from 700 to 900°F with an exhaust stack inside diameter of 7.122 inches. Additionally a proposed gas turbine exhaust four-nozzle eductor system was constructed for testing under high temperature conditions to verify temperature correlation parameters developed using cool air as the primary flow medium. A secondary air flow metering box was designed and partially completed for the determination of eductor pumping characteristics during hot flow operations.

TABLE OF CONTENTS

LIST OF FIGURES

LIST OF TABLES

NOMENCLATURE

English Letter Symbols

A	-	Area, ft^2
AFR	-	Air to fuel ratio
B	-	Atmospheric pressure, in Hg absolute
c	-	Sonic velocity, ft/sec
c_d	-	Discharge coefficient
d	-	Downstream diameter or restriction diameter
D	-	Upstream diameter
f	-	Frequency (Hz)
F	-	Area factor for thermal expansion
g_c	-	Proportionality factor in Newton's Second Law, 32.174 lbm-ft/lbf-sec^2
h	-	Enthalpy, Btu/lbm
k	-	Ratio of specific heats, for air = 1.40
L	-	Length, ft
LHV	-	Lower heating value of fuel, 18,100 Btu/lbm for No. 2D diesel fuel
m	-	Mass, lbm
$\dot{m}$	-	Mass rate of flow, lbm/sec
P	-	Pressure
R	-	Gas constant, for air = 53.34 ft-lbf/lbm-°R
T	-	Temperature, °F, °R
U	-	Velocity, ft/sec
Y	-	Venturi tube expansion factor

Dimensionless Groupings

M - Mach number

Re - Reynolds number

Greek Letter Symbols

β - Diameter ratio, d/D

μ - Absolute viscosity, $lbf\text{-}sec/ft^2$

ρ - Density, lbm/ft^3

Subscripts

1 - Exhaust nozzle number 1

2 - Exhaust nozzle number 2

3 - Exhaust nozzle number 3

4 - Exhaust nozzle number 4

a - air

A - ambient air

B - Burner or combustor

BB - Blanked side of nozzle box

d - discharge

e - Exhaust or eductor nozzle

F - Fuel

g - Entrance nozle gauge

N - Entrance nozzle

R - Fuel recirculation line

SH - Stack horizontal thermocouple

SV - Stack vertical thermocouple

V - Venturi

Tabulated Data

PEH - Stack exhaust pressure relative to atmospheric, in Hg

PNH - Entrance nozzle upstream pressure relative to atmospheric, in Hg

ΔPN - Pressure difference across entrance nozzle, in H_2O

PPL - Pitot tube static pressure relative to atmospheric, in H_2O

ΔPP - Pressure difference across pitot tube, in H_2O

ΔPT - Pressure difference between entrance nozzle upstream tap and nozzle box entrance tap, in Hg

PUH - U-Bend upstream pressure relative to atmospheric, in Hg

ΔPU - Pressure difference across U-bend, in H_2O

PVH - Venturi upstream pressure relative to atmospheric, in Hg

ΔPV - Pressure difference across Venturi, in Hg

ACKNOWLEDGMENT

The work herein reported has been supported by the Naval Sea Systems Command, Code 0331. The understanding, guidance and interminable patience of Professor Paul F. Pucci, the author's thesis advisor, was an inestimable source of inspiration and reassurance throughout the project. The assistance and ingenuity provided by the personnel of the Department of Mechanical Engineering machine shop is also sincerely appreciated.

I. INTRODUCTION

The increasing use of gas turbines as the primary propulsion power plant for modern naval vessels is a trend which has developed in recent years and apparently will continue into the immediate future. With the compactness and high performance of these power plants have come the inevitable problems associated with relatively high mass flow rates and escalating operating temperatures. Air to fuel mass flow ratios four to five times those for conventional steam propulsion plants and combustion gas temperatures in the neighborhood of 900 degrees Fahrenheit (°F) have combined to create two problems of particular significance. Sensitive mast mounted electronics aboard modern naval vessels are particularly susceptible to continuous elevated temperature exposure, and the large exhaust mass flows at these elevated temperatures create an infrared plume which is a prime target for heat seeking offensive weapons.

One means of lowering the combustion gas or primary flow temperature is through the introduction of cool ambient or secondary air into the exhaust flow with thorough mixing before ejection into the atmosphere. An exhaust gas eductor system, such as is employed on the DD-963 class destroyers, provides a simple, effective and relatively lightweight apparatus which accomplishes this task without an unacceptable degradation of gas turbine performance.

Although considerable effort has gone into the examination of single-nozzle eductor systems, it has been only recently that attempts have been made to improve eductor efficiency through the use of multiple nozzle systems. Pucci [1] demonstrated that the performance of an eductor is primarily dependent upon the completeness of mixing of primary and secondary flows and that the degree of mixing is a function of mixing stack length, mixing stack cross-sectional area to primary nozzle area ratio and secondary to primary flow-rate ratio.

Ellin [2] conducted model tests of the four-nozzle eductor in use aboard the DD-963 class destroyers as well as several proposed configurations using compressed as as the primary flow medium. He established base line cold air performance data for the existing system and demonstrated that the variable having the greatest effect upon eductor performance was the mixing stack area to primary nozzle area ratio. Moss [3] and Harrell [4], also using cold air as the primary flow medium, investigated multiple-nozzle system performance as a function of geometry and reported improved pumping characteristics for several geometric configurations. Throughout these studies there was an implied dependence of eductor performance upon the primary flow temperature. This temperature dependence has been accounted for by utilizing a temperature correlation parameter based upon the theoretical kinetics in the mixing stack.

The major objective of this project is to construct a combustion gas generator which can be used to validate this correlation parameter at primary flow temperatures near those encountered under actual operating conditions. The added complexities of constructing models for high temperature operation necessarily limit the number and variety of geometric configurations which could reasonably be examined. However, a wide variety of eductor geometries can readily be accomodated under cold flow conditions. Of these, the most promising can then be modeled for hot flow testing.

Additionally, the combustion gas generator is adaptable for examination of other items peculiar to gas turbine exhaust systems such as turning vanes, silencers and varying stack geometries.

II. DESIGN

The necessary ingredients for the generation of combustion gas obviously include an air supply, fuel supply and a means of obtaining combustion. However, the overriding consideration throughout the design effort was to insure that the combination of equipment utilized would yield a system which was reasonable in size for the modelling to be accomplished. The availability of an operational Boeing Model 502-6A gas turbine engine raised the question of whether or not the burner can and igniter assembly might be utilized to provide the source of combustion. Further investigation indicated that the nozzle box itself might provide a convenient means of coupling the burner can to the exhaust stack. Additionally, the 8.250 inch outside diameter (OD) of the nozzle box discharge was a reasonable stack diameter lying about midway between the stack diameters used by Harrell and Moss [3 and 4]. It was necessary at this point to determine the flow requirements of the system and verify the compatibility of the Boeing turbine components.

A. EXHAUST STACK OPERATING REQUIREMENTS

Utilizing existing DD-963 uptake design drawings [5] the velocities of the primary flow were determined to be turbulent ($Re \simeq 10^5$). Consequently, turbulent momentum exchange is the predominant mechanism characterizing primary flow and kinetic and internal energy considerations dominate

viscous effects. Since Mach number (M) can be shown to represent the square root of the ratio of the kinetic energy of a flow to its internal energy, it is a more significant parameter than Reynolds number in describing the primary flow through the stack. Similarity of Mach number was therefore used to model the primary flow. Using dimensional data and mid-range mass flow data from the DD-963 uptake design [5] it was determined that a primary flow Mach number of 0.07 would provide a reasonable stack flow characterization. From LM2500 turbine performance data [6] a mid-range exhaust gas temperature (T_e) of 850 °F was chosen.

1. Mass and Energy Balance

To determine the air and fuel mass flow requirements of the gas generator an energy balance was first carried out to fix the air to fuel mass ratio (AFR):

Energy of Air + Energy of Fuel = Energy of Exhaust + Losses.

For a first approximation losses were neglected so that

$$\dot{m}_a h_a + \dot{m}_f h_f = (\dot{m}_a + \dot{m}_f) h_e . \qquad (1)$$

Dividing equation (1) by $\dot{m}_f$ and substituting the fuel lower heating value for h_f expresses the energy balance in terms of the air to fuel ratio as follows:

$$(AFR)\ h_a + LHV = (AFR)\ h_e + h_e.$$

$$AFR = \frac{LHV - h_e}{h_e - h_a} . \qquad (2)$$

Since air to fuel ratios are generally quite high the exhaust gas can be assumed to be characterized primarily as air at the exhaust temperature and

$$h_e \simeq h_a \text{ @ } 850°F.$$

Using an LHV = 18,100 BTU/lbm [7] and assuming that the incoming air would be supplied by an air compressor with a nominal discharge temperature of 150°F the enthalpy values can be found from the Gas Tables [8]. Then h_a = 151 Btu/lbm at 150°F, h_a = 320 Btu/lbm at 850°F and the

$$AFR = 105 .$$

Mass continuity must also be maintained so that

$$\dot{m}_a + \dot{m}_f = \dot{m}_e .$$

The AFR can be used to eliminate $\dot{m}_f$ so that

$$1.01\ \dot{m}_a = \dot{m}_e . \qquad (3)$$

The exhaust gas mass flow rate can be expressed in terms of the gas density (ρ_e), the area of the exhaust stack (A_e) and the exhaust gas velocity (U_e) as follows [9]:

$$\dot{m}_e = \rho_e A_e U_e . \qquad (4)$$

For the isentropic flow of a perfect gas [9],

$$\rho_e = \frac{P_e}{R T_e} , \qquad (5)$$

$$U = MC = M(g_c k R T_e)^{0.5} , \qquad (6)$$

and

$$A_e = \frac{\pi D_e^2}{4} \qquad (7)$$

where D_e is the diameter of the exhaust stack ($\simeq$ 8.0 inch), P_e is the exhaust stack pressure (assumed to be slightly above atmospheric or about 31 inches of mercury absolute), c is the sonic velocity in the exhaust gas and T_e is the exhaust temperature. Combining equations (4), (5), (6) and (7) gives

$$\dot{m}_e = \left(\frac{P_e}{R T_e}\right)\left(\frac{\pi D_e^2}{4}\right) M (g_c k R T_e)^{0.5}$$

or

$$\dot{m}_a = 1.35 \text{ lbm/sec.}$$

From the air to fuel ratio

$$\dot{m}_f = 46.2 \text{ lbm/hr.}$$

2. Turbine Component Compatibility

Technical data for the Boeing gas turbine engine [10] rated the turbine burner fuel nozzle for 66.5 lbm/hr at 100 psig. The maximum fuel mass flow rate to the turbine was 230 lbm/hr at full power. It was therefore concluded that the fuel mass flow requirements were well within the capabilities of the Boeing engine components. It also appeared that certain fuel system components such as the high pressure fuel pump, fuel supply pump, fuel filter and fuel shut off solenoid valve could also be considered for use in the model's fuel system.

B. AIR SYSTEM

The availability of a Carrier model 18P350 centrifugal air compressor previously used for jet engine studies proved to be more than adequate for providing the primary air mass flows required. With an output rating [11] of 4.8 lbm/sec at 240°F and 29.5 psia the Carrier compressor was capable of providing more than 3.5 times the necessary air flow. An additional convenience was the existing physical arrangement of the compressor. Discharge air was piped underground to a separate building and exhausted through an 8 inch inside diameter (ID) flanged horizontal pipe with an

8" butterfly-type shutoff valve and a 4 inch globe-type bypass valve. See Figure 1. It was also possible to regulate the compressor discharge mass flow using an atmospheric bleed valve installed on the compressor itself.

1. Valve and Piping Arrangement

The nozzle box consisted of a formed torroidal stainless steel can designed to collect the burner combustion gas and direct flow through a set of stationary nozzles into the compressor turbine. If the compressor shaft were removed the remaining four inch diameter hole could be used to provide cooling air for temperature regulation to the exhaust stack as shown in Figures 2 and 3.

The physical dimensions of the turbine nozzle box with its 4 inch ID entrance throat size made it convenient to use 4 inch ID piping for the air distribution system. It was necessary, however, to insure that the area reduction from the 8 inch ID compressor discharge pipe would not result in choked flow and thereby limit the air mass flow rate. For isentropic, ideal compressible gas flow through a restriction the maximum mass flow rate ($\dot{m}_{max}$) possible is given by [9]

$$\dot{m}_{max} = 0.686\ A^{*}P_{o}(g_{c}/RT_{o})^{0.5}$$

where A^{*} is the area of the restriction, P_{o} is the stagnation pressure and T_{o} is the stagnation temperature. For a 4 inch

ID restriction under temperature and pressure conditions at the compressor discharge,

$$\dot{m}_{max} = 8.03 \text{ lbm/sec}$$

which was a factor of six above the air mass flow required. Therefore it was decided to use locally available 4 inch ID aluminum tubing.

It was also desired to provide an independent air flow control capability for both the burner inlet and the bypass air through the center of the nozzle box. This would improve air mass flow distribution control and provide a means of regulating exhaust stack temperature. Commercially available 4 inch ID butterfly-type valves with motor controllers were chosen to enable operation from a remote control panel. Two additional hand operated valves of the same type were also felt necessary to increase system flexibility and provide a local means of regulating compressor discharge mass flow. Figure 4 shows the piping and valve arrangement decided upon.

2. Entrance Nozzle

An entrance transition piece was necessary to mate the 8 inch ID compressor discharge piping with the 4 inch ID system piping as shown in Figure 4. This nozzle arrangement with an area ratio of 4:1 could also be used to measure inlet air mass flow if properly calibrated.

3. Bypass Air Mixer

Since combustion gas leaving the burner would enter the stack through the fixed nozzles around the outside of the nozzle box discharge with a counterclockwise swirl, some means must be provided to force mixing with the bypass air entering through the center of the nozzle box. A bypass air mixer was designed to force bypass air radially outward into the combustion gas flow but with an opposite swirl. Figures 2, 3, 5 and 6 indicate mixer construction and location in the nozzle box. The resulting cross sectional area of the mixer flow channel (A_m) was slightly less than the area of the 4 inch supply piping. For this reason it was necessary to verify that choking would not occur in the mixer. The maximum flow rate ($\dot{m}_{max}$) is again given by [9]

$$\dot{m}_{max} = 0.686\ A^* P_o (g_c/RT_o)^{0.5} \qquad (8)$$

with A^*, P_o and T_o evaluated as described in Section II.B.1. It is assumed that temperature losses along the inlet pipe are relatively small and T_o = 150°F. Since the exhaust stack pressure is slightly above atmospheric (≈ 31 in Hg), P_o at the mixer can be found from the relationship

$$\frac{P^*}{P_o} = 0.528$$

and the maximum flow rate is

$$\dot{m}_{max} = 7.24 \text{ lbm/sec}$$

which is well in excess of the 1.35 lbm/sec required.

4. Exhaust Stack

Commercially available 8 inch OD 0.250 inch wall thickness (WT) grade 304 stainless steel tubing was chosen for the exhaust stack for its availability, dimensional compatibility with the nozzle box discharge diameter and high temperature characteristics.

C. FUEL SYSTEM

As described in Section II.A.1., the majority of the fuel system could be provided from the existing Boeing turbine fuel system components. In fact the only remaining requirements were a fuel storage capability, a prime mover for the high pressure fuel pump which was gear driven on the Boeing turbine and some means of conveniently regulating fuel pressure to the burner. Since the mass flow rate contemplated was the equivalent of about 6.5 gallons per hour (gph) it was felt that a 55 gallon commercial drum could be used for fuel storage without requiring an inordinate replenishment frequency. The general fuel system arrangement is detailed in Figure 7.

1. High Pressure Fuel Pump

The Boeing Gas Turbine Engine high pressure fuel pump was to be coupled to an AC motor. Reference 10 specified a fuel pump rating of 100 lbm/hr at 1800 revolutions per

minute (rpm) and a discharge head of 300 psig. Although no pump efficiency (η_p) was provided, $\eta_p = 0.8$ was considered reasonable with a considerable margin for error. The power required by a motor with an assumed efficiency (η_m) of 0.8 is given by [12]

$$\text{POWER} = \frac{2.31\ \dot{m}_f\ (P_F - P_S)}{\eta_P\ \eta_m}$$

where $(P_F - P_S)$ represents the head pressure (psig). Using the pump rating data

$$\text{POWER} = 0.055 \text{ horsepower.}$$

A locally available 0.5 Horsepower 110 volt, alternating current (AC) synchronous induction motor was therefore chosen to be direct coupled to the existing turbine high pressure fuel pump. The constant 15 psig inlet head pressure required was provided by utilizing the 24 volt direct current (DC) motor driven fuel supply pump furnished with the turbine for that purpose.

2. Fuel Pressure Control

A simple means of providing fuel pressure control by recirculating pump discharge through a regulating valve back to the pump suction was considered adequate. The recirculation line and control valve were sized to be at least as large as the pump suction line to provide a full

range of discharge pressure adjustment. The control system arrangement is shown in Figure 7.

D. EDUCTOR SYSTEM

The eductor system was designed to model the system investigated by Moss with the object of obtaining correlation data and verifying the temperature correlation parameter used in the cold flow studies. Figure 8 indicates the general eductor system arrangement.

1. The Mixing Stack

The choice of locally available 7.5 inch OD 0.188 inch WT steel pipe was compatible with the exhaust stack diameter and more easily machined than stainless steel. The ratio of the measured average ID of 7.122 inches for this pipe with the measured mixing stack diameter used by Moss of 11.700 inches fixed the dimensional scale factor at 0.6087. It was intended to test the 3 diameter long (21.866 inch) mixing stack initially and then the 2 diameter (14.244 inch) long stack which could be machined from the 3 diameter stack.

2. Eductor Nozzles

The four nozzle geometry used by Moss was scaled maintaining the ratio of mixing stack diameters. Moss' mixing stack to total nozzle area ratio of 3:1 and nozzle length to diameter ratio of 1.225:1 were also utilized. The nozzle elements were designed to be machined from steel tubing and welded to a circular nozzle plate which would bolt onto the exhaust stack. The nozzle inlets were to be

machined to a 0.500 inch radius to smooth transition flow. This arrangement would facilitate nozzle changing in the event other geometries were to be tested. Figures 9 and 10 provide nozzle assembly details.

3. Eductor Air Metering Box

Since eductor performance is sensitive to secondary air flow of disturbances, a measurement of secondary air flows using the restrictive flow measuring devices commercially available is impractical. For this reason a large metering box was designed to enclose the entire eductor assembly and act as an air plenum. A set of standard ASME long radius flow nozzles of varying cross-sectional areas were chosen to be mounted in the metering box away from the eductor. A characteristic eductor pumping curve could then be obtained by successively plugging these secondary flow nozzles and measuring the corresponding plenum vacuum. Extrapolation of this curve in non-dimensional form could be used to find the pumping characteristics of the eductor in an open configuration [2].

The metering box was designed with interchangeable stack seal plates to enable variation of both exhaust and mixing stack sizes up to 1 foot in diameter. The seal plates also have a limited range of vertical movement to facilitate exhaust and mixing stack alignment. The entire box was designed to be movable along an angle iron track parallel to the gas generator stack longitudinal centerline. This would enable variation of the mixing stack to nozzle separation

distance without adjustment and realignment of the mixing stack. The mixing stack end plate was also designed to be movable to allow centering for various mixing stack lengths. Flow straighteners made of sixteen mesh wire screen were provided between the secondary air inlet and the eductor and an access door was added for eductor adjustment. The metering box general arrangement is pictured in Figure 11 and a dimensional layout is given in Figure 8.

E. INSTRUMENTATION

It was desired to keep instrumentation simple, yet pertinent and utilize readily available commercial equipment as much as possible. The term "principle measurement" designates those quantities which must be known in order to fully determine the experimental objective. Operational measurements are those desired to provide supplemental information concerned with the operation of the gas generator. Since the follow-up objective of this project will be to obtain eductor pumping data, sufficient capability was designed into the instrumentation to allow for the additional pressure and temperature measurements required for eductor performance evaluations. These requirements will not, however, be treated further in this report. The general arrangement and location of temperature and pressure instrumentation are detailed in Figure 13.

1. Principle Measurements

The determination of the exhaust stack Mach number and temperature requires an evaluation of the total mass

flow rate ($\dot{m}_a + \dot{m}_f$), the pressure in the exhaust stack and the exhaust stack temperature. Fuel mass flow was to be measured utilizing a Cox Instrument model V40-A vortex flowmeter coupled with an Anadex Instruments model CPM-603 frequency counter. This resulted in a useable flow range from 11.2 to 280.0 lbm/hr. The flowmeter was to be installed in the fuel system as shown in Figure 7.

Air mass flow was to be determined by measuring the pressure drop across the entrance air nozzle (ΔPN) and the air temperature at the nozzle inlet (T_N). Four-point averaging pressure taps were to be located both upstream and downstream of the entrance nozzle. A bank of eight Meriam Instrument model M-108 fifty inch well-type manometers was to be used to monitor pressure readings. Four manometers utilizing mercury (Hg) as the indicating fluid and 4 utilizing water (H_2O) were to be connected through a combination of high pressure, low pressure and atmospheric valve manifolds as detailed in Figures 12 and 13. This arrangement would enable the matching of pressure levels to a manometer of appropriate output range without rearranging the interconnecting tubing. Entrance nozzle temperature was to be measured, as were all low temperatures, utilizing copper-constantan Thermcouple probes wired to a Newport model 267A digital pyrometer capable of monitoring 18 inputs through a barrel-type selector switch.

Exhaust stack (T_e) and all other high temperature measurements were to be made with chromel-alumel thermocouple

probes wired to a second Newport model 267A digital pyrometer. Exhaust stack pressure (PEH) was measured through a four-point averaging pressure tap located one stack ID upstream of the eductor nozzle entrance.

2. Operational Measurements

Burner exhaust temperature had to be monitored to protect the system from overheating. It was also considered desirable to measure the pressure drops across the burner inlet U-bend (ΔPU) and from the entrance nozzle inlet to the nozzle box inlet (ΔPT) in order that an estimate of the individual mass flows through the burner and nozzle box bypass could be calculated. Additional fuel system instrumentation is shown in Figure 7.

F. ELECTRICAL SYSTEM

The instrumentation and equipment planned in the design required a source of 110 volt AC and 24 volt DC power. This was to be provided through the electrical distribution system detailed in Figure 14. The DC power supply was to be incorporated into a central control panel which would also house the pressure tap valve manifolds, mass flowmeter readout, low temperature thermocouple readout and the power control switches for the electrically operated equipment.

High voltage to the burner can igniter plug and glow coil was to be supplied from the Boeing turbine points set which could be powered from the 24 volt DC supply.

III. CONSTRUCTION

In general individual component manufacture and assembly was accomplished as specified in Section II. Since no major design modifications were required during construction and critical dimensional data have already been specified, additional detail of the assembly process would not be particularly elucidating for the purposes of this report. Therefore further remarks concerning construction and assembly will be confined to a discussion of those items either not anticipated during the design process or which manifest themselves as useful changes. Figure 15 gives the major dimensional layout of the gas generator. Figures 16 through 27 pictorially describe the completed system.

A. INSULATION

To reduce radiation heat losses along the exhaust stack one inch of fiberglass insulation encased within an aluminum sheath was installed as pictured in Figure 17. An asbestos lined aluminum heat shield, shown in Figure 22, was added between the burner can and the bypass air piping. Since the bypass air control valve employed rubber seating surfaces of unknown temperature resistance characteristics, some heat isolation was considered prudent. To protect the bypass air valve seat from conducted heat propagated through the nozzle box and connecting piping, asbestos gaskets were inserted on both sides of the valve.

B. FUEL DRAINAGE

In the event ignition was not immediately achieved raw fuel would collect in the bottom of the nozzle box and in the exhaust stack itself. A fuel drain system pictured in Figure 17 was installed to prevent fuel accumulation during the starting process.

C. FUEL PRESSURE CONTROL

A remote control rod was attached to the fuel pressure control valve enabling fuel pressure control from the system operating station.

IV. CALIBRATION

The use of pressure drop data across various nonstandard air line restrictions for the calculation of mass flow rates required that these restrictions be calibrated to a known standard. In particular, this involved calibration of the entrance nozzle and U-bend pressure taps. Additionally, the fuel mass flowmeter characteristics needed to be defined under operational conditions. Thermocouple calibration was not considered necessary since these instruments have a history of reliability within the manufacturer provided specifications and the planned temperature measuring arrangement provided sufficient redundancy to enable in-service cross-checks.

A. ENTRANCE NOZZLE CALIBRATION

The entrance nozzle calibration arrangement is detailed in Figure 28 and pictured in Figure 29. An ASME standard Herschel-type Venturi [13] was used as the primary flow measuring device. The pitot tube was installed to enable a rough verification of the Venturi data. Tabulated data recorded over a range of inlet air flow rates are shown in Tables I, II and III. For the Venturi used the corresponding mass flow rate is given by [13]

$$\dot{m}_a \text{ (lbm/sec)} = 0.099702\, C_d\, Y\, d^2\, F(1-\beta^4)^{-0.5}(\rho h_w)^{0.5} \qquad (11)$$

where C_d is the discharge coefficient of the Venturi, Y is the expansion factor, d is the throat diameter (in.), F is the area thermal expansion factor, β is the ratio of throat diameter to entrance diameter, ρ is the denstiy of the fluid and h_W is the differential pressure (in. H_2O). Table IV summarizes the results of calculations for the data of Tables I, II and III and Figure 30 is the calibration curve obtained. This calibration curve gave sufficient mass flow estimates for the operation of the gas generator. The dimensional data obtained and plotted in Figure 30 were put into non-dimensional form, for detailed analysis employing a discharge coefficient defined from equation (11) as

$$C_{DN} = \frac{\dot{m}_a (1 - \beta_N^4)^{0.5} (\rho h_W)^{-0.5}}{0.099702\ Y\ d^2\ F}$$

with the corresponding parameters evaluated at the entrance nozzle. F was assumed equal to 1.0 for this computation. Corresponding Reynolds numbers were also determined and the resulting data are tabulated in Table V and displayed graphically in Figure 31. Sample calculations are detailed in Appendix A. It should be noted that for the operational range expected ($Re_{DN} \approx 1.8 \times 10^5$) C_{DN} is virtually constant with varying Re_{DN}. The increase in C_{DN} at high Reynolds numbers was caused by choking in the Venturi at these mass flow rates.

B. U-BEND CALIBRATION

U-bend calibration was accomplished by varying the burner air supply valve position with the bypass air valve closed and maintaining a constant setting on the inlet valve to the entrance nozzle. The entrance nozzle inlet valve was adjusted to give a ΔPN near the expected operating point of the gas generator with the burner supply valve wide open. The calibration run was then repeated with a new setting of the initial ΔPN. Mass flow rates were then found from the entrance nozzle calibration curve. Tabulated data for runs with an initial ΔPN of 8.8 and 9.7 inches of water are recorded in Table VI. Table VII summarizes the resulting mass flow rates and Figure 32 displays these results graphically.

C. MASS FLOWMETER CALIBRATION

The mass flowmeter was calibrated by using the fuel supply pump to discharge fuel through a control valve into a container positioned upon a scale. The time required to pump a specified weight of fuel at a constant mass flowmeter frequency was used to calculate a mass flow rate for that flowmeter frequency. This process was repeated for a range of flows. The data are tabulated in Table VIII and the results summarized in Table IX and graphically displayed in Figure 33. The calibration curve is linear as was expected.

V. OPERATION

Ignition and sustained combustion were obtained with virtually no difficulty. A short period of operation during which various control elements were cycled through their operating ranges was sufficient to characterize the system as having a wide range of operation and being extremely stable at a given operating point.

A. START UP

An AFR of 20 in the burner was chosen as a reasonable set point for attempting initial ignition. This was near the ideal stoichiometric ratio of 15 and was a recommended ignition point [14]. A fuel mass flow rate setting of 40 lbm/hr (113 Hz) was chosen for attempting ignition. This value was close to that predicted for the 850°F operating point. Using an AFR of 20 and the U-bend calibration curve (Figure 32) the corresponding ΔPU was about 1 inch of H_2O. Both the bypass air and burner supply air valves were set wide open and the compressor discharge bypass valve was adjusted to give a ΔPU of 1 in H_2O. The fuel supply pump and high pressure fuel pump were started and the fuel pressure was set to minimum (35 psig). The igniter plug and glow coil were energized and allowed to operate for about 10 seconds before fuel was admitted by energizing the solenoid opening the fuel shutoff valve. Immediately after opening the fuel shutoff valve, fuel pressure was raised until a

frequency of 113 Hz was reached on the mass flowmeter output. Ignition occurred and was self sustaining after the igniter plug and glow coil were deactivated. The burner can discharge temperature rapidly exceeded the 1300°F maximum recommended in the Boeing operating manual [10]. Closing the bypass air valve to a 40% open position immediately reduced burner temperature to a stable 1000°F. (Closing the bypass air valve increased the upstream pressure and forced more air through the burner.) It was found that simply by controlling the bypass air valve setting exhaust temperatures varying from 500 to 700 °F could be obtained. Burner temperature (T_B) was naturally extremely sensitive to the bypass air setting. Assuming that the supply air compressor is in operation the following is a recommended starting sequence:

1. Energize main power panel, thermocouple and mass flowmeter readouts.
2. Open both bypass air and fuel supply air valves 100%.
3. Set the high temperature thermocouple selector switch to read burner can temperature (T_B).
4. Open the compressor discharge bypass valve until the pressure difference across the U-bend (ΔPU) reads 1 inch of water.
5. Energize the fuel supply pump and insure a discharge pressure of 14 to 16 psig is reached.
6. Open the fuel control valve 100% (minimum pressure).
7. Energize the high pressure fuel pump and adjust the fuel pressure to 60 psi (A 5 psig drop in fuel pressure will occur when the fuel shutoff valve is opened.)

8. Energize the igniter plug and allow to operate for approximately 10 seconds.

10. Open the fuel shutoff valve.

11. As soon as ingition is obtained deactivate the igniter. (If combustion is not sustained immediately close the fuel shutoff valve and allow the system to purge for 2 minutes. Begin again with step 8.)

12. Begin closing the bypass air valve immediately while monitoring burner temperature (T_B). Continue closing the bypass air valve until T_B stabilizes. (Do not allow burner temperature to exceed 1300°F.)

13. Adjust the bypass air valve to obtain a burner temperature of 1200°F.

The critical starting parameters are summarized under the start column in Table X. The most important item in the starting sequence is to begin closing the bypass air control valve immediately upon obtaining sustained combustion. The burner exhaust temperature will rise very rapidly after ignition and the AFR must be increased correspondingly to avoid a temperature overshoot.

B. STEADY STATE OPERATION

Burner can exhaust temperature is dependent upon the AFR in the combustion can which is effected by the setting of the fuel pressure, the bypass air control valve, the burner supply air control valve and the compressor discharge valve. Thus, the combination of various valve settings to obtain a given exhaust stack temperature and Mach number is not unique. However, a full range of control is possible with the burner supply valve left wide open. It is relatively easy once sustained combustion has been obtained to reach a desired operating point using the following procedure:

1. Adjust the compressor discharge bypass valve to give the ΔPN corresponding to the mass flow rate for the Mach number desired.

2. Increase fuel pressure until either the desired exhaust stack temperature is reached or T_B reaches 1200°F.

3. If T_B reaches 1200°F before the desired T_e is reached close the bypass air valve until T_B is reduced to 1000°F.

4. Readjust the compressor discharge bypass valve to obtain the correct mass flow setting and begin again with step 2.

It was found in practice that this procedure would enable a stack temperature variation of over 200°F while maintaining a constant Mach number mass flow setting and could be accomplished with less than three compressor discharge valve adjustments. If it is desired to reduce the exhaust stack temperature, fuel pressure can be lowered until either the required stack temperature is reached or the burner temperature drops to 700°F. The bypass air valve can now be opened to raise burner temperature and further lower stack temperature but the compressor discharge valve must be readjusted to maintain the desired mass flow. It is expected that sustained combustion will cease for air to fuel ratios in the neighborhood of 10 to 15 in the burner can. Although the intended operating points are nowhere near this value of AFR, the minimum air mass flow rates and corresponding pressure drops can be determined from the calibration curves for various fuel settings.

Table X gives a listing of parameter values which gave a range of exhaust stack temperatures based upon estimated

air and fuel mass flows required for a Mach number of 0.07. Follow-up analysis, detailed in Appendix B, determined that the Mach number was actually 0.08. However, it is evident that these temperatures may easily be obtained for a Mach number of 0.07 through fuel and air flow adjustment. Table XI reduces the data of Table X utilizing an entrance nozzle discharge coefficient (C_{DN}) of 0.9175. Reynolds numbers at the entrance nozzle were calculated and found to be in the neighborhood of 1.7×10^5 which is in the flat range of Figure 31.

1. Fuel Pressure Calibration

During the process of gathering operational data, a range of fuel pressures was obtained with corresponding mass flowmeter frequency readings. These data are plotted on Figure 33 and enable an approximate adjustment of fuel mass flow using fuel pressure readings. This is particularly convenient during starting and when shifting operating points over wide ranges.

2. Exhaust Nozzle Temperature Profiles

A set of horizontal and vertical exhaust nozzle temperature profiles were obtained using the thermocouple traverse arrangement picture in Figure 27. The supply air compressor discharge temperature tended to creep upward during the period when data were taken. This resulted in a corresponding increase in burner temperature and exhaust stack temperature. Therefore the data, tabulated in Tables XII through XV and

presented graphically in Figures 34 through 41 were normalized using the maximum temperature. It should be noted that temperatures tended to be high toward the centerline of the exhaust stack and that in general the maximum temperature did not occur at the nozzle center.

VI. DESIGN VERIFICATION

Although the original design was for a Mach number of 0.07 the reduced operating point data corresponded to a Mach number of 0.08. It was therefore necessary to recompute the theoretical flow requirements in order that a valid comparison could be made. It was also possible, at this point, to further refine the theoretical predictions by utilizing exact dimensional information and the temperatures and pressures actually encountered. With this information, an estimate of the losses, previously ignored, could also be made.

A. THEORETICAL FLOW PREDICTION

The theoretical mass flow requirements were calculated using the same procedure discussed in Section II.A.1. In this case the compressor discharge temperature was taken to be 174°F. An average exhaust stack temperature of 850°F and an exhaust stack pressure of 31.9 inches Hg were also utilized. This resulted in a predicted AFR of 105.

A mass balance using 7.122 inches for the stack diameter, a Mach number of 0.08 and a specific heat ratio of 1.36 resulted in a theoretical air mass flow of 1.234 lbm/sec and a fuel mass flow of 42.3 lbm/hr. The difference between predicted and actual air to fuel ratios was about 13%.

B. ACTUAL FLOW RATE COMPARISON

The actual total mass flow measured ($\dot{m}_a + \dot{m}_f = 1.276$ lbm/sec) was greater than that predicted ($\dot{m}_a + \dot{m}_f = 1.246$) theoretically by 2.5%. This was to be expected since the design was based upon the assumption of a perfect gas with ideal isentropic compressible flow. No attempt was made to account for friction or temperature losses in the piping and the combustion efficiency of the burner can was not considered. From the geometry of the system it is apparent that piping losses may be significant.

The difference between the mid-stack temperature and the eductor nozzle temperature ($T_e - T_{SH}$) indicated that there was a substantial heat loss along the stack even with the installed insulation. Additionally the difference in temperature across the nozzle box ($T_B - T_{BB}$), which was not insulated, indicated appreciable heat loss through radiation and convection. Finally, the value of T_e used in the calculation was an average of the four nozzle centerline temperatures. As previously discussed, the centerline temperatures were less than the maximum temperatures for all four nozzles and the actual temperature tended to vary both above and below the centerline temperature. Therefore the T_e used was not necessarily representative of the energy-averaged bulk temperature.

C. MACH NUMBER AND TEMPERATURE SIMILARITY

The primary design objective was to obtain a Mach number of 0.07 at an exhaust stack operating temperature of

850°F. Evaluation of operational data verified that the gas generator was capable of meeting this objective as well as a wide range of operating points both above and below this setting. The fuel and mass flow control systems proved sufficiently flexible to enable system operation over a much wider range than was initially envisioned.

VII. CONCLUSION

The objective of this project was to provide an operational combustion gas generator which could be used to model gas turbine exhaust systems. A secondary objective was to model the eductor nozzle configuration used by Moss while maintaining Mach number similarity and generating temperatures which would duplicate those encountered in actual service.

It was verified that operating temperatures of 850°F could be generated and maintained at Mach numbers matching those utilized in the Moss cold flow studies. In fact, a much wider range of operating points was found possible facilitating system useage for gas turbine stack modelling under various other operating conditions.

The system proved to be stable, repeatable and relatively simple to operate. All system control and data display equipments were accessible from a central operating station.

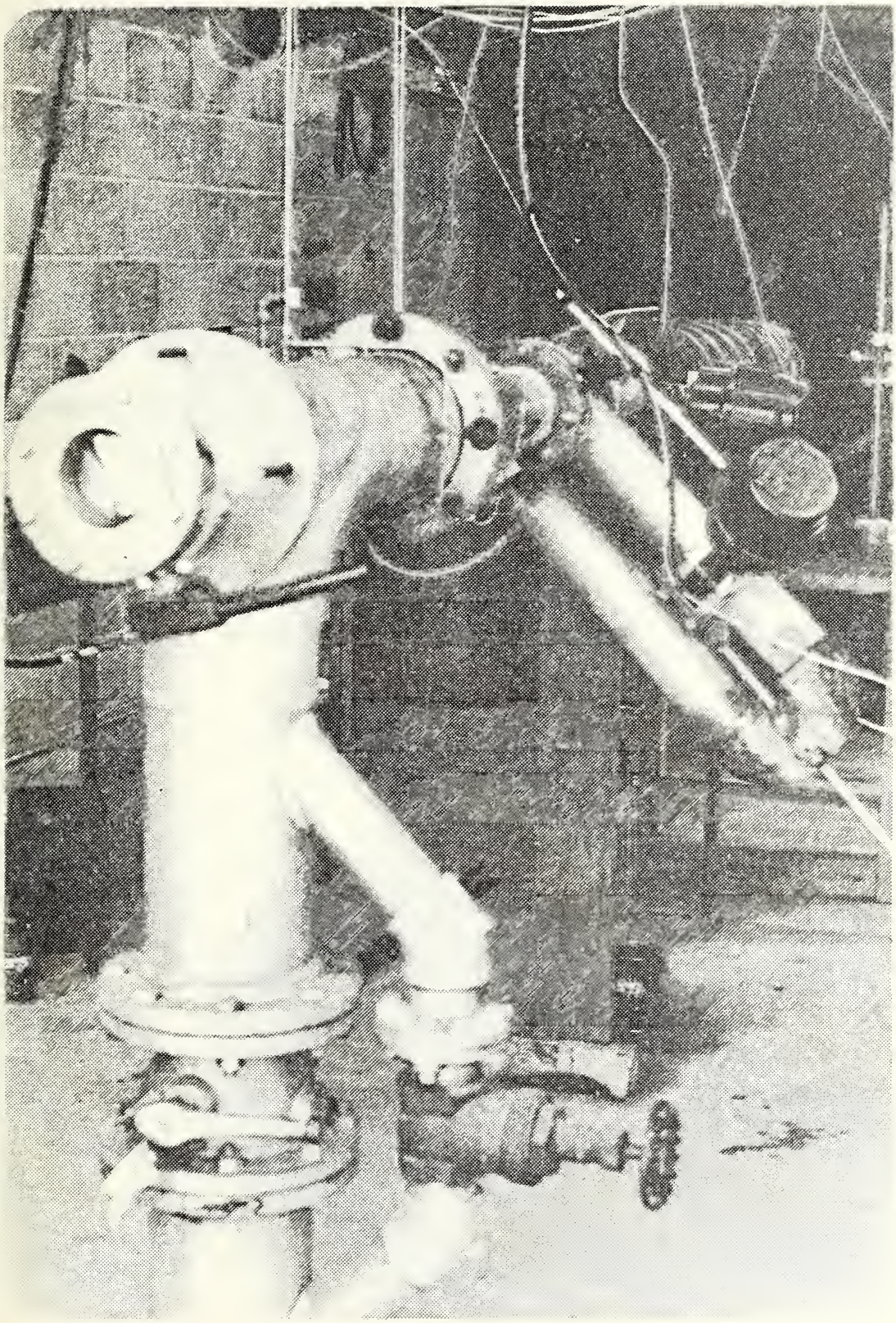

FIGURE 1. Air Supply Compressor Discharge Arrangement

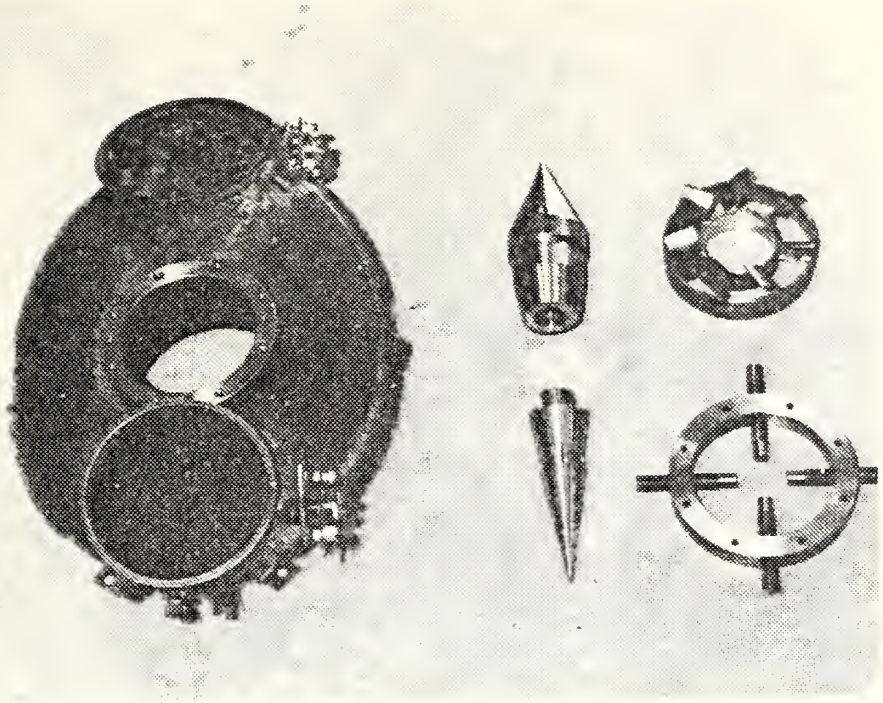

FIGURE 2. Nozzle Box and Bypass Air Mixing Assembly

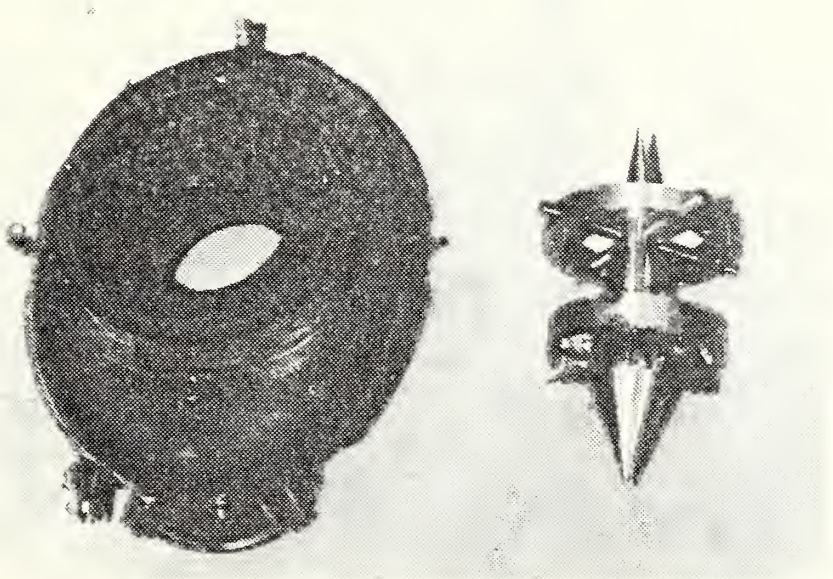

FIGURE 3. Nozzle Box Reverse and Assembled Bypass Air Mixer

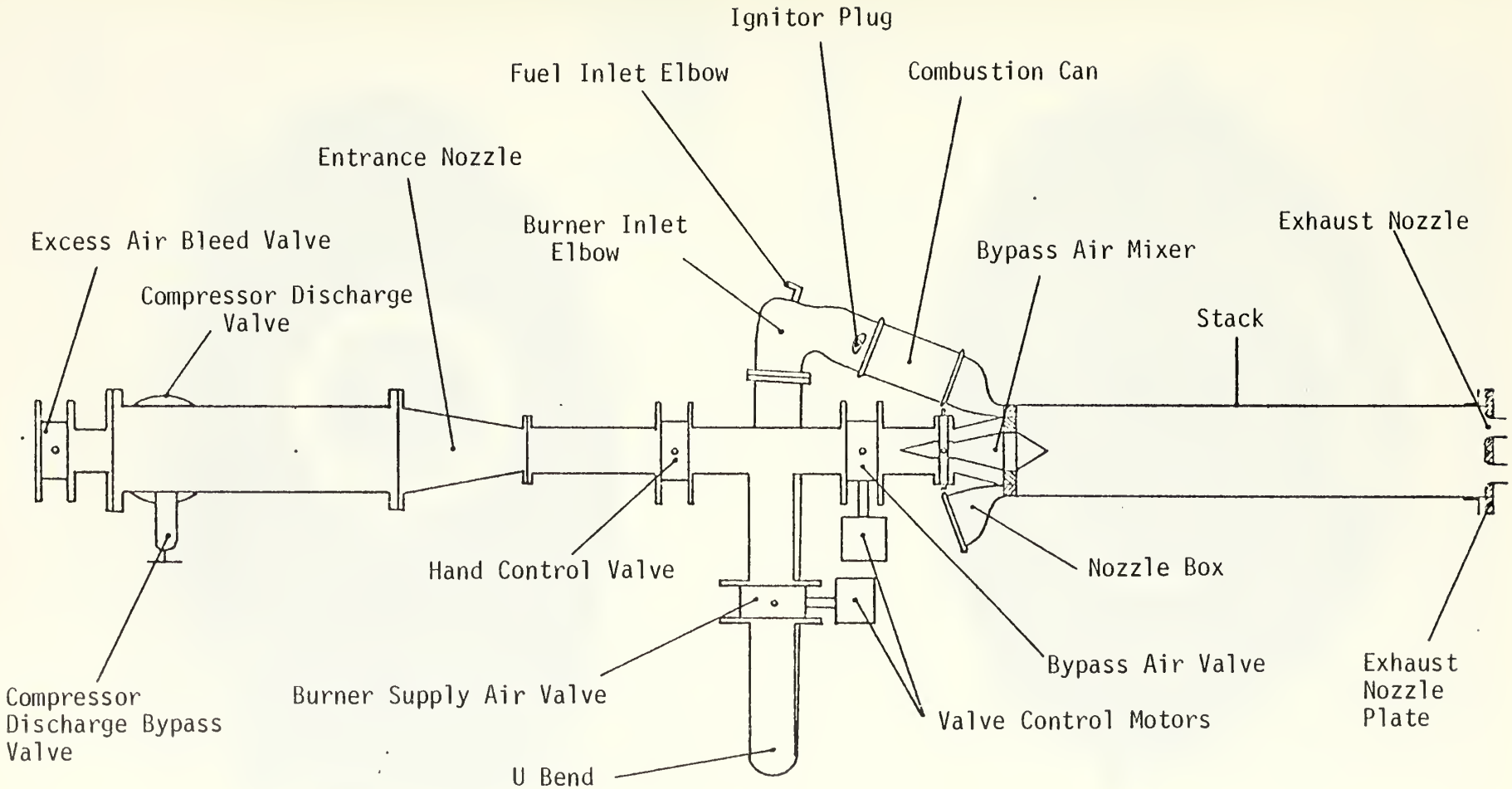

FIGURE 4. Gas Generator Nomenclature and Arrangement

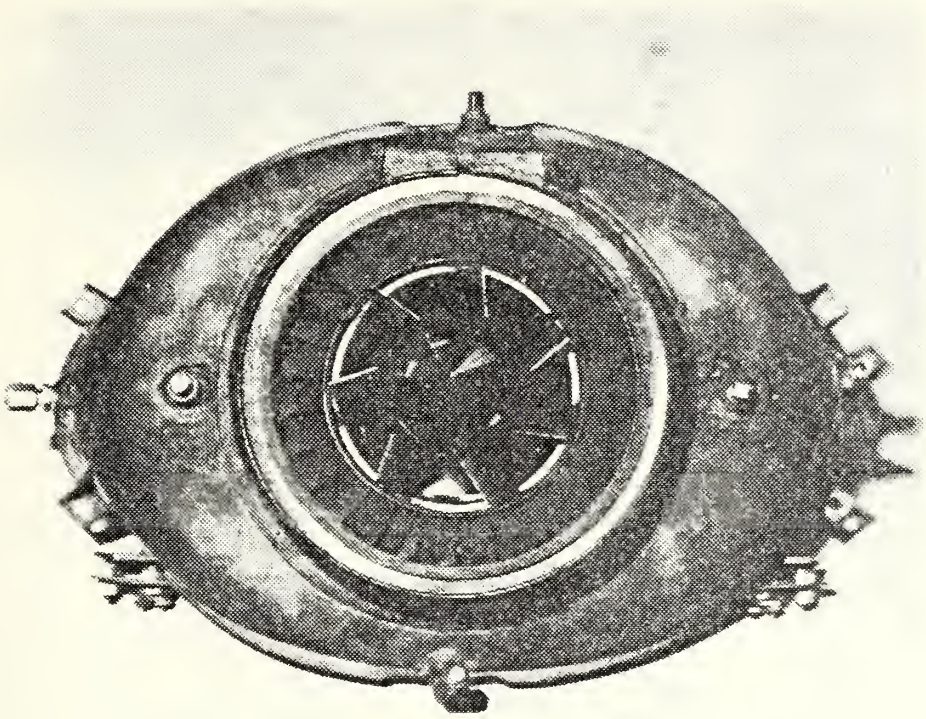

FIGURE 5. Nozzle Box Discharge Side with Mixer

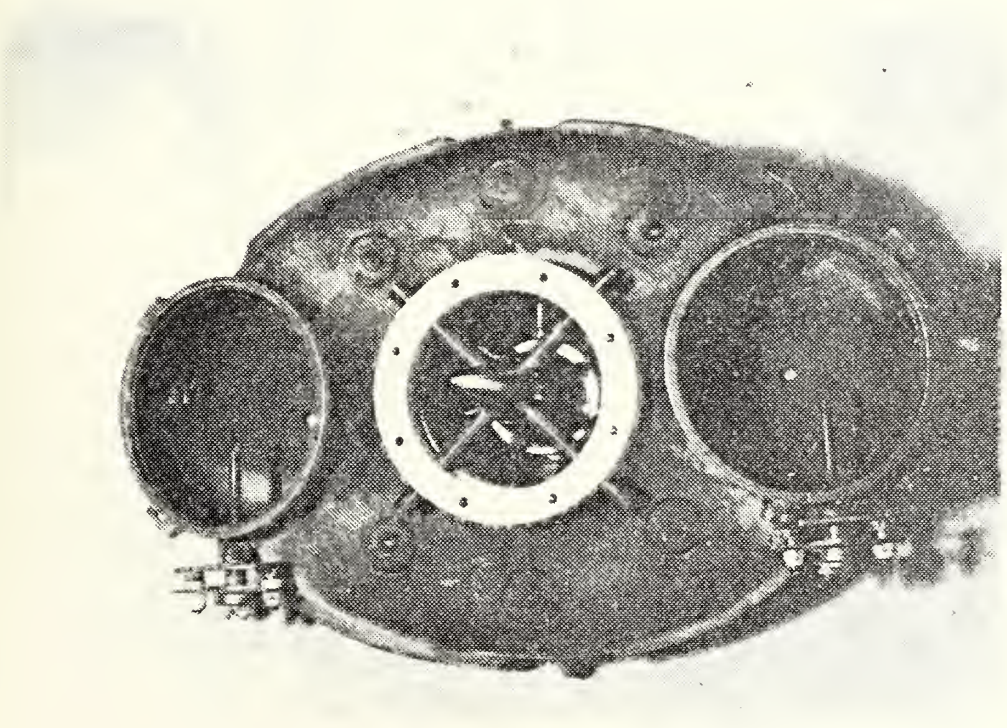

FIGURE 6. Nozzle Box Inlet Side with Mixer

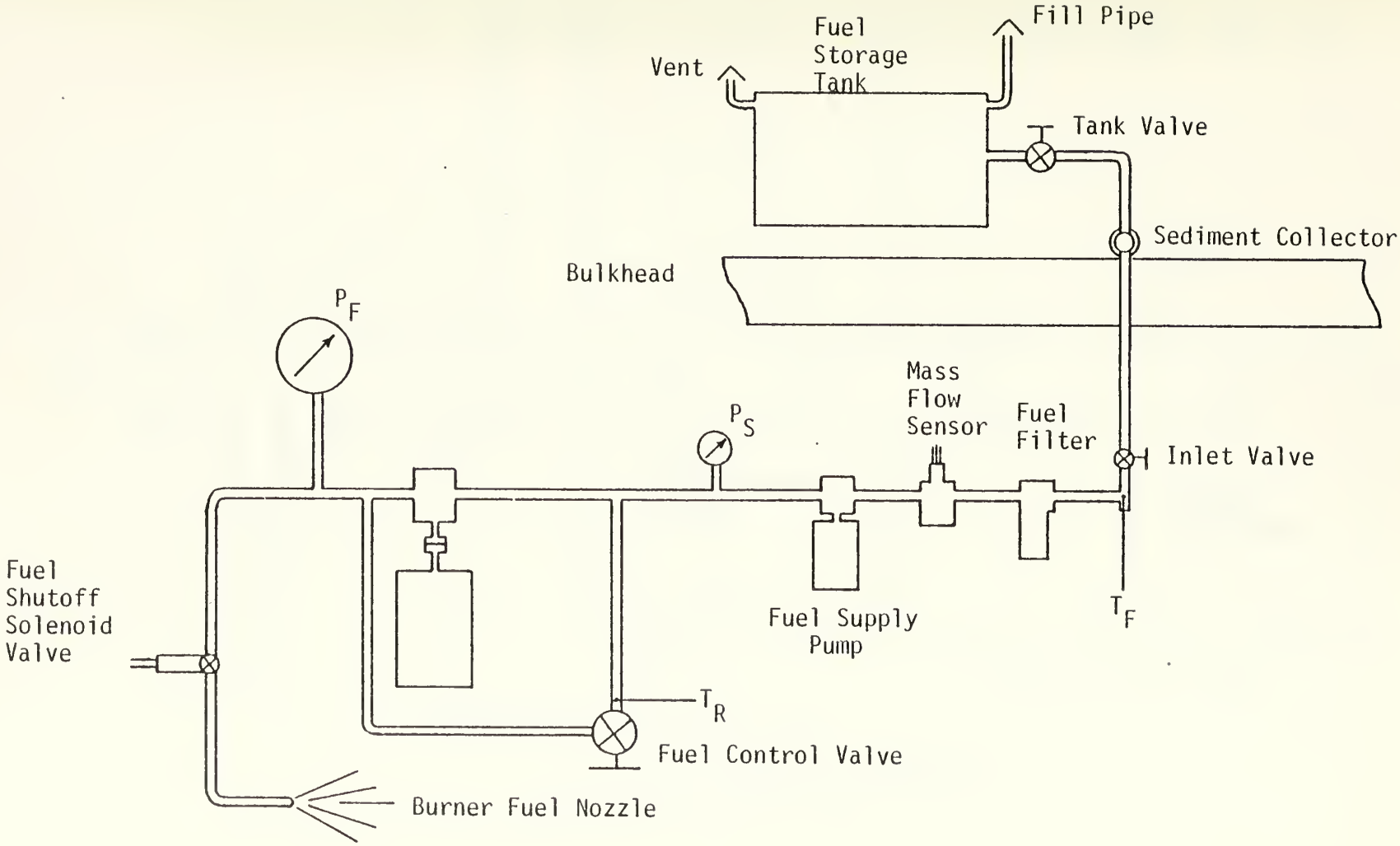

FIGURE 7. Gas Generator Fuel System

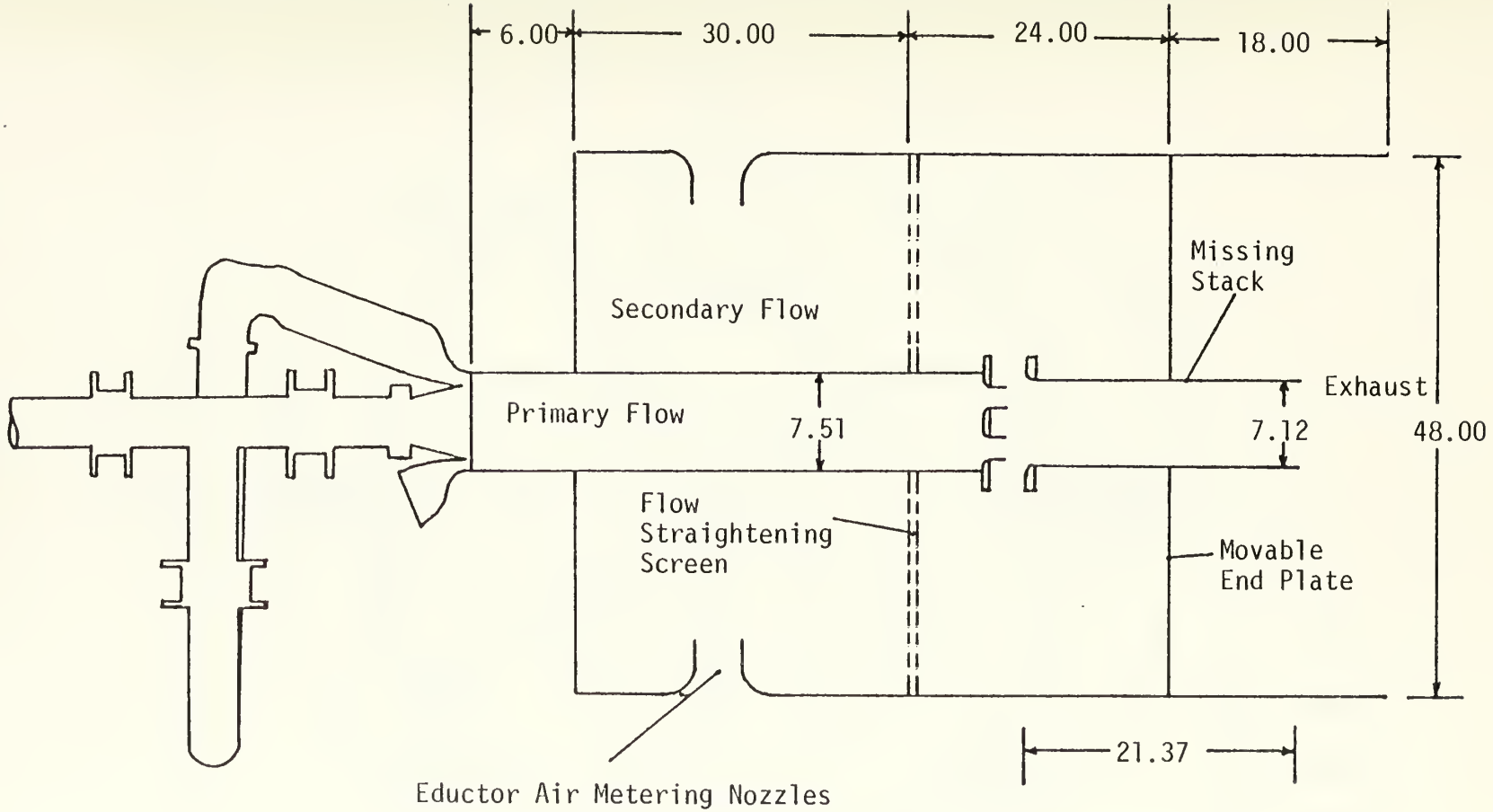

Overall box dimensions: 48x48x72

All dimensions in inches.

FIGURE 8. Eductor Air Metering Box Arrangement

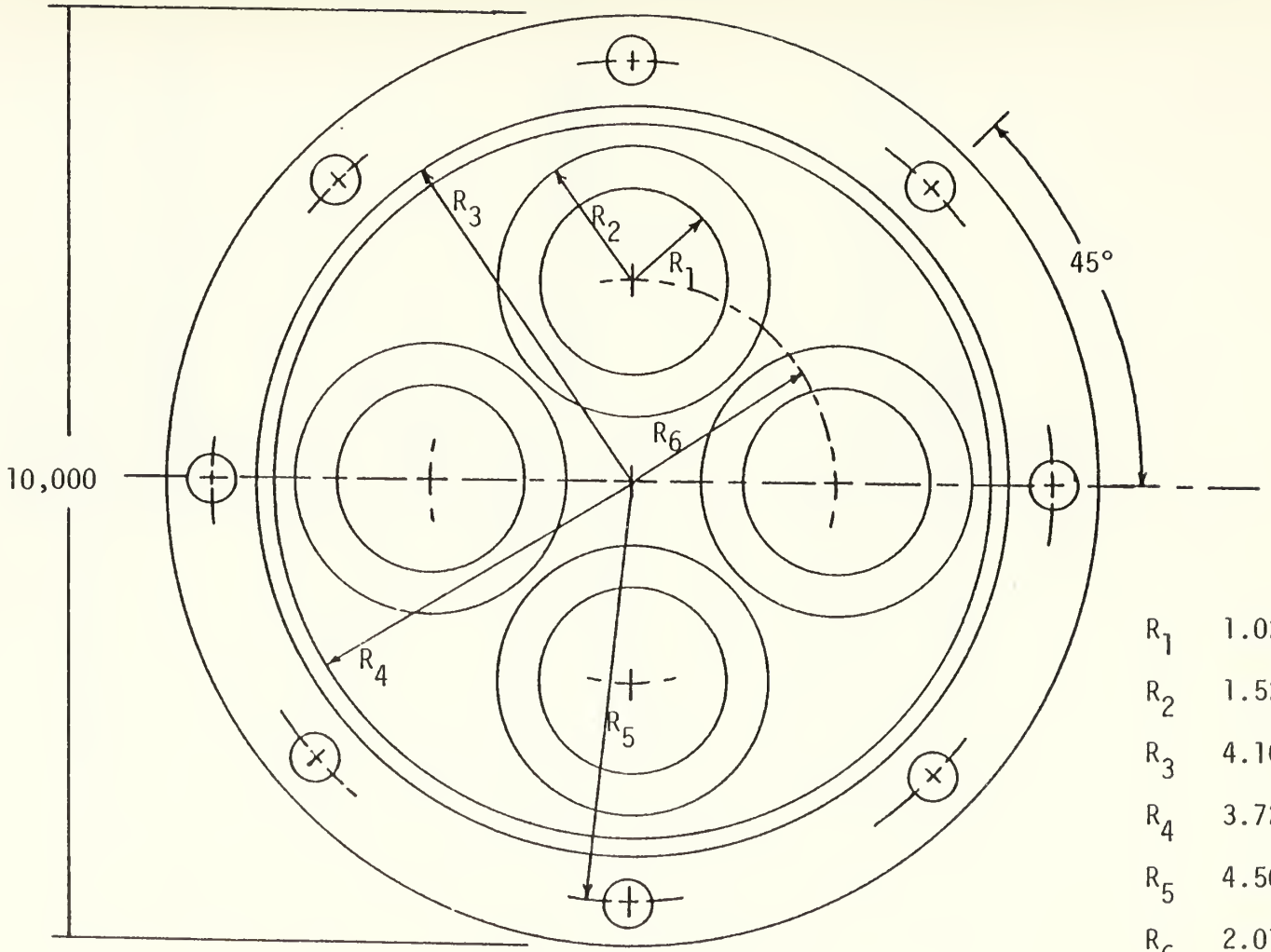

R_1	1.029
R_2	1.529
R_3	4.108
R_4	3.729
R_5	4.509
R_6	2.070

FIGURE 9. Exhaust Nozzle Plate Plane View

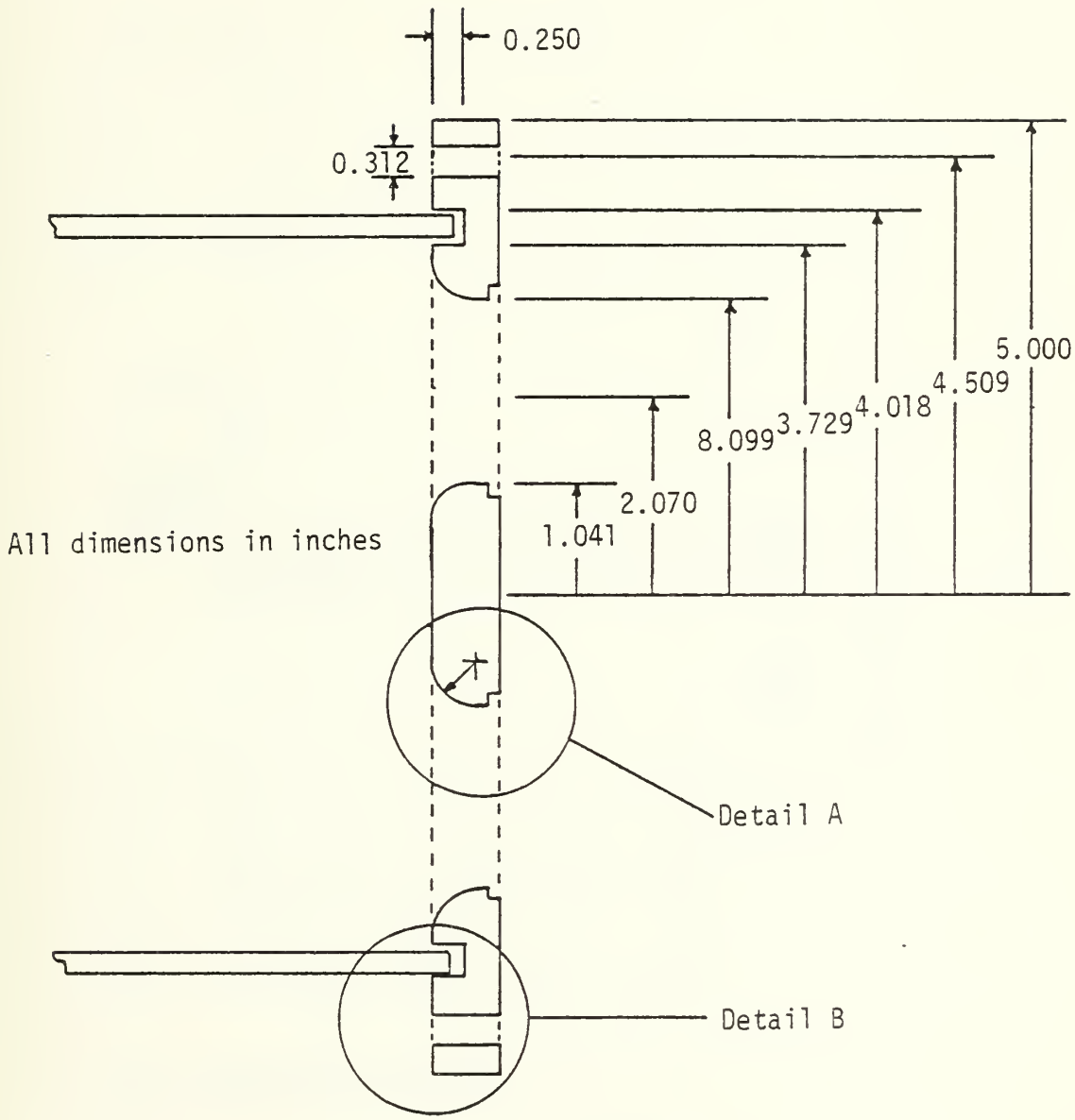

FIGURE 10. Exhaust Nozzle Plate Side View

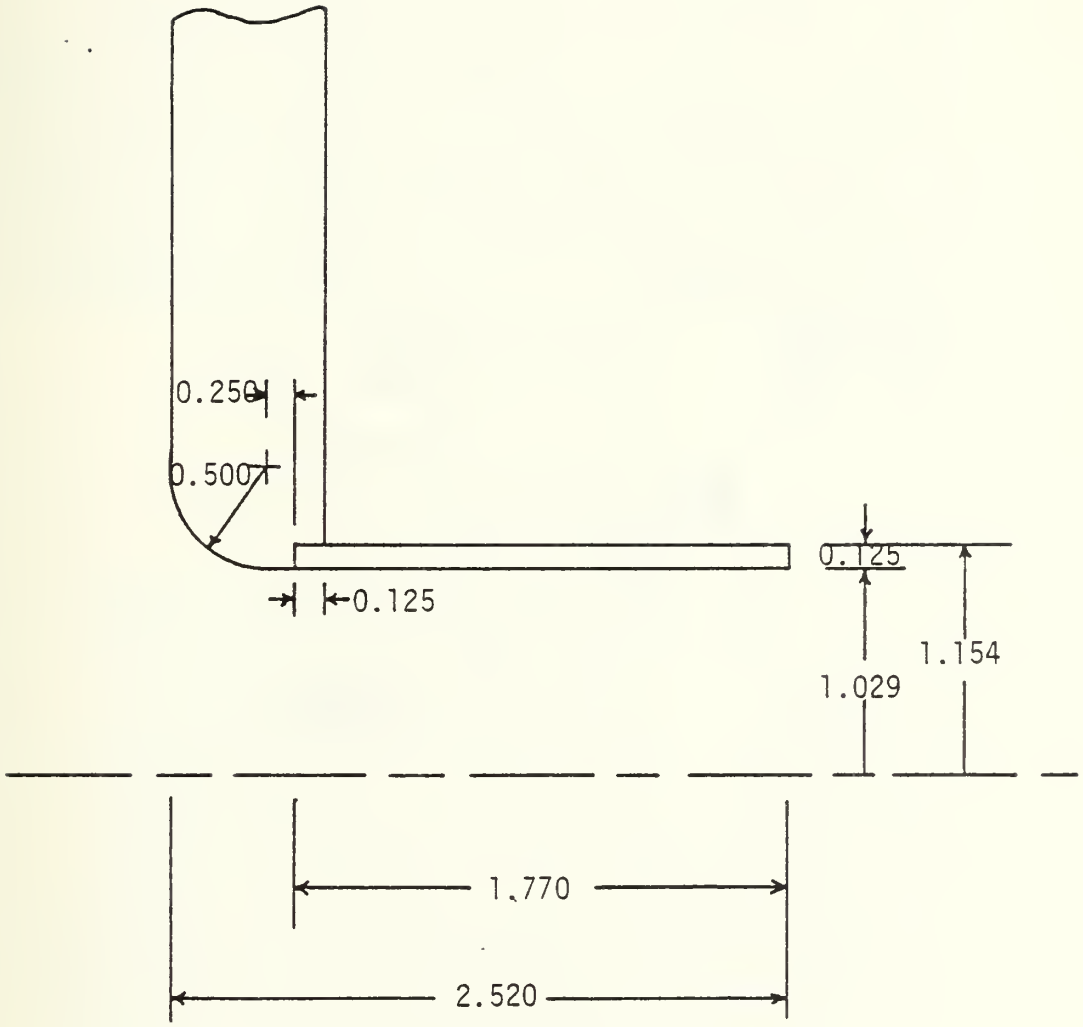

All dimensions in inches

FIGURE 10. Continued. Detail A

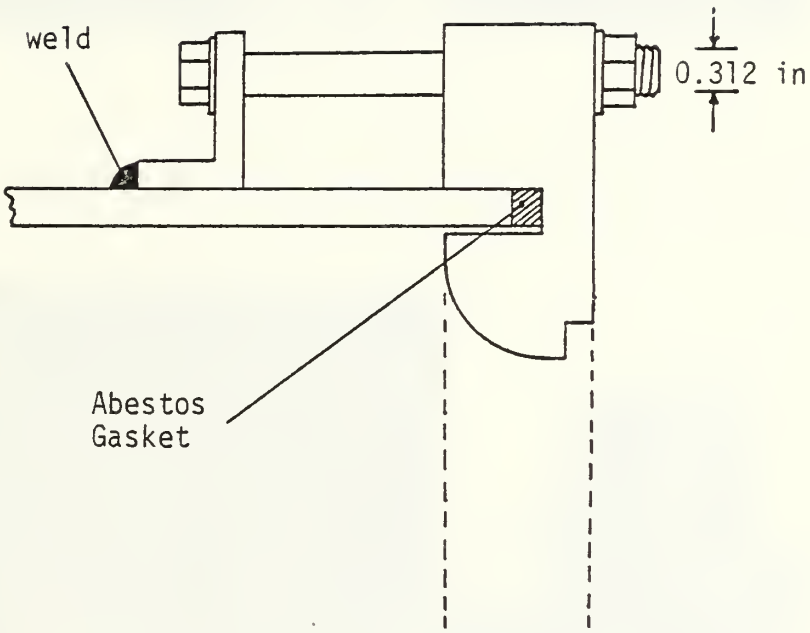

FIGURE 10. Continued. Detail B

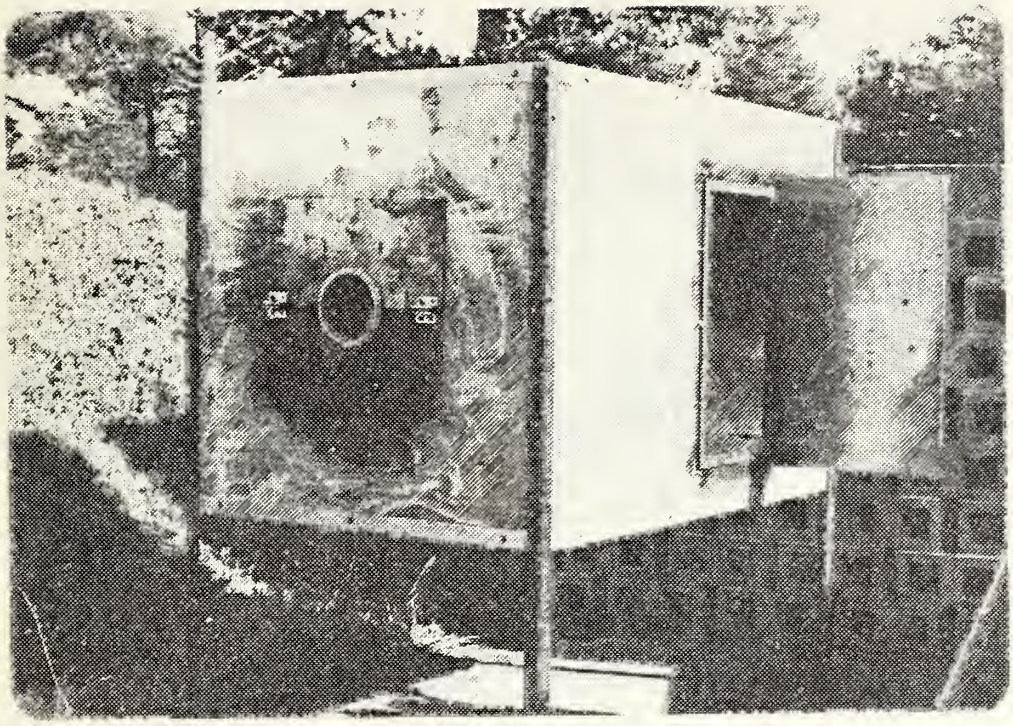

FIGURE 11. Secondary Air Flow Metering Box Without Flow Nozzles

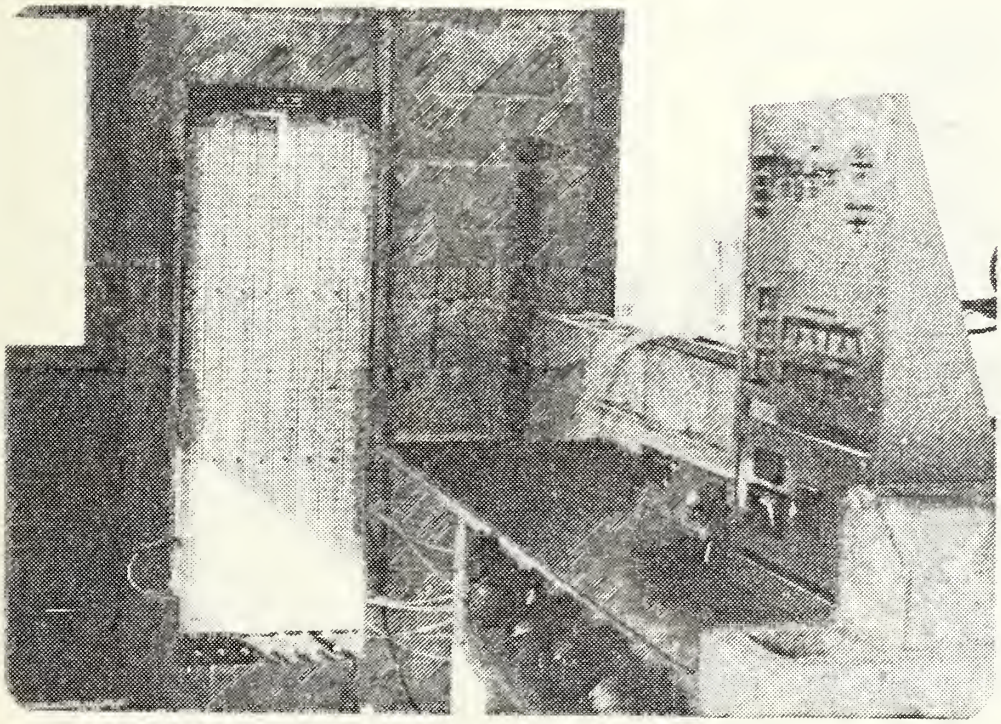

FIGURE 12. Gas Generator Instrumentation and Control Equipment

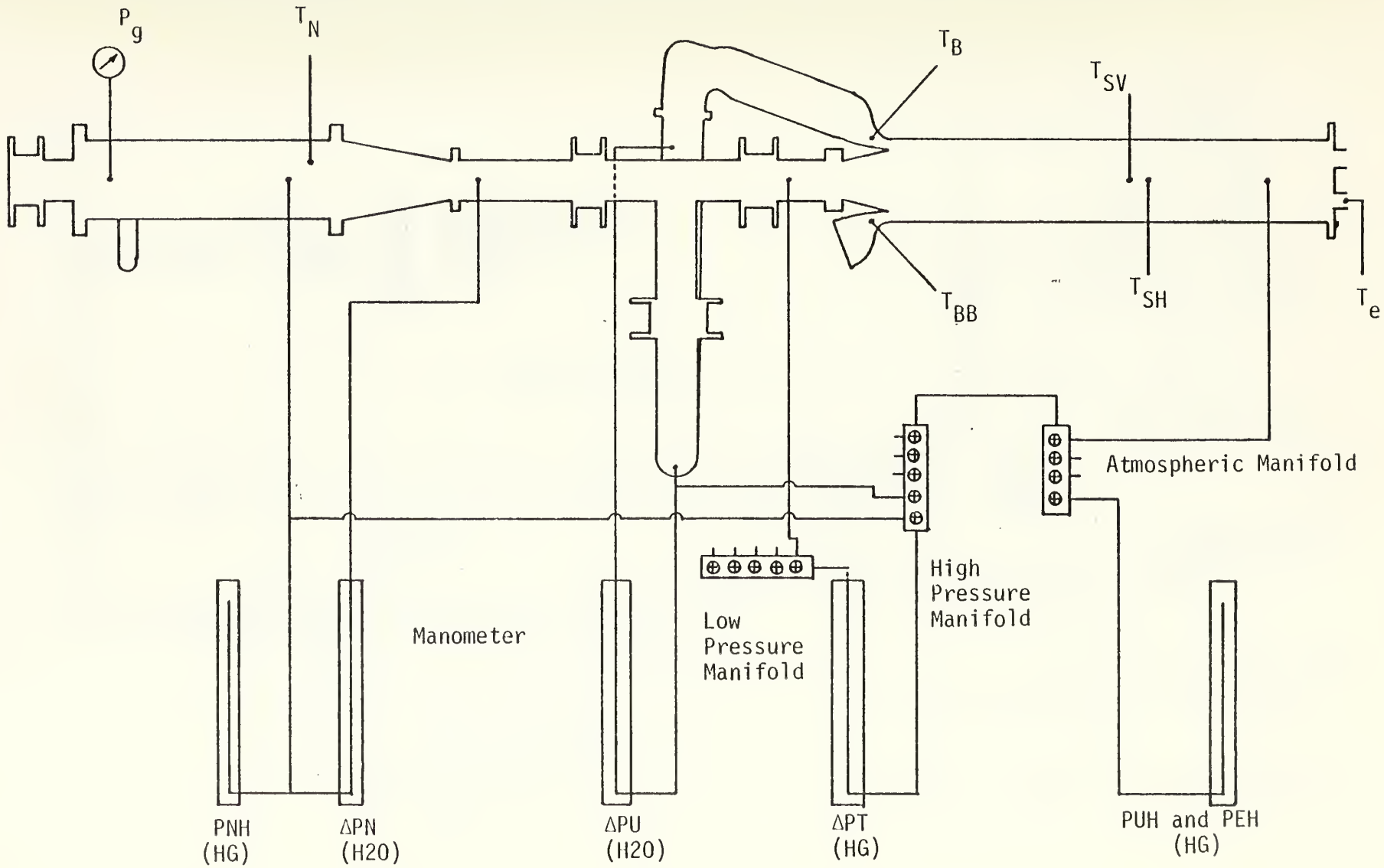

FIGURE 13. Gas Generator Pressure Reading and Thermocouple Arrangement

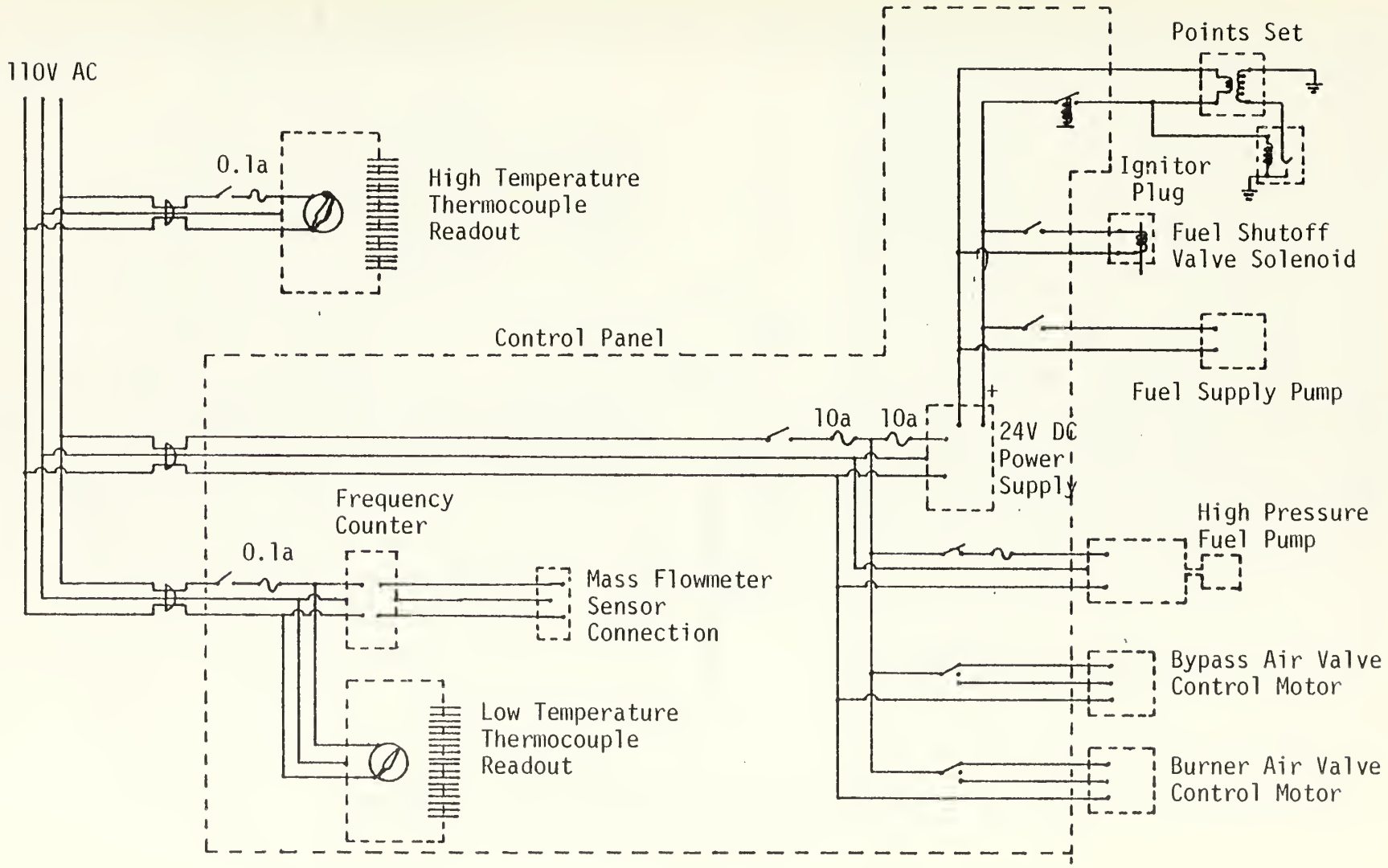

FIGURE 14. Gas Generator Electrical System

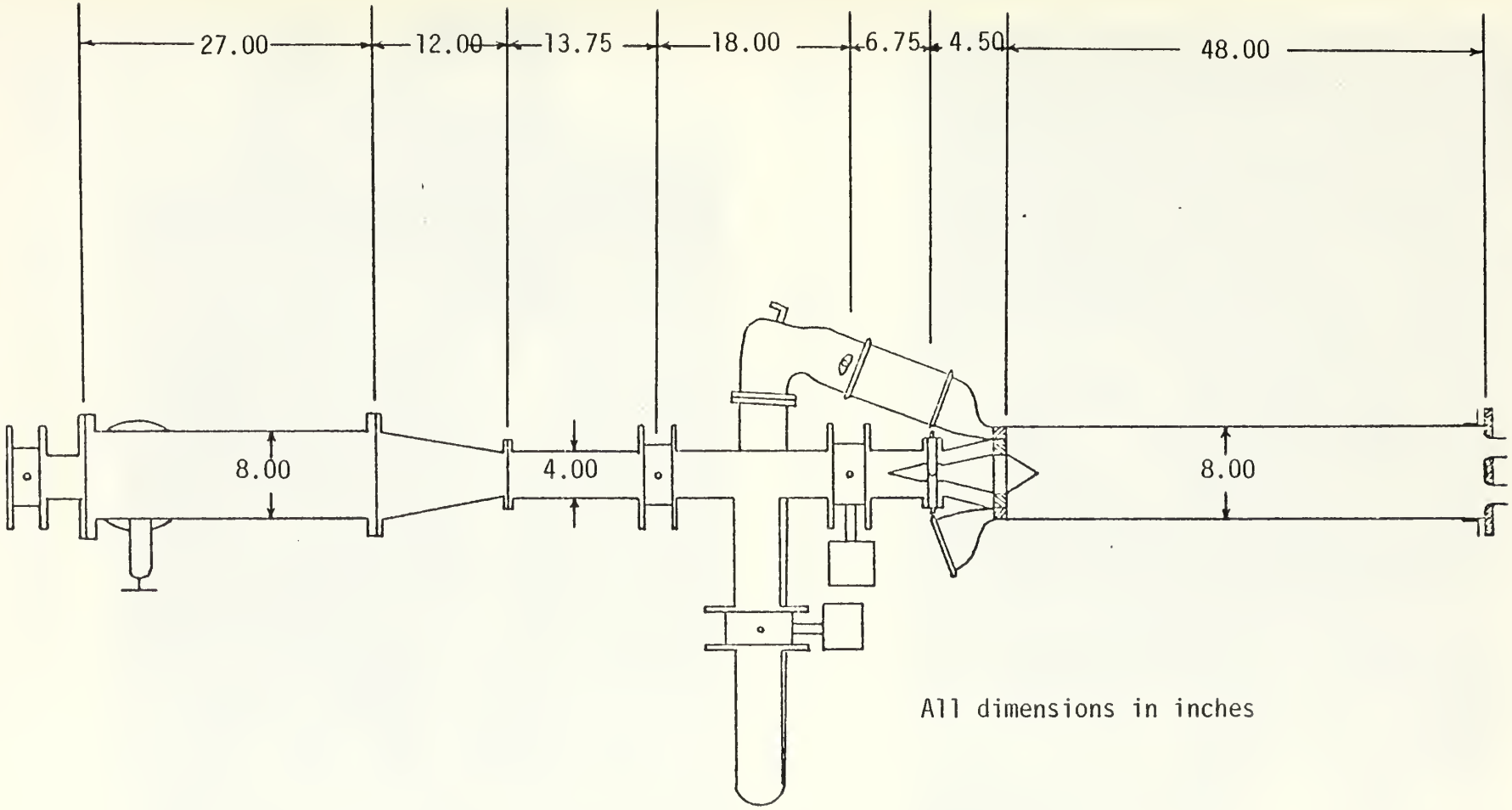

FIGURE 15. Gas Generator Dimensional Layout

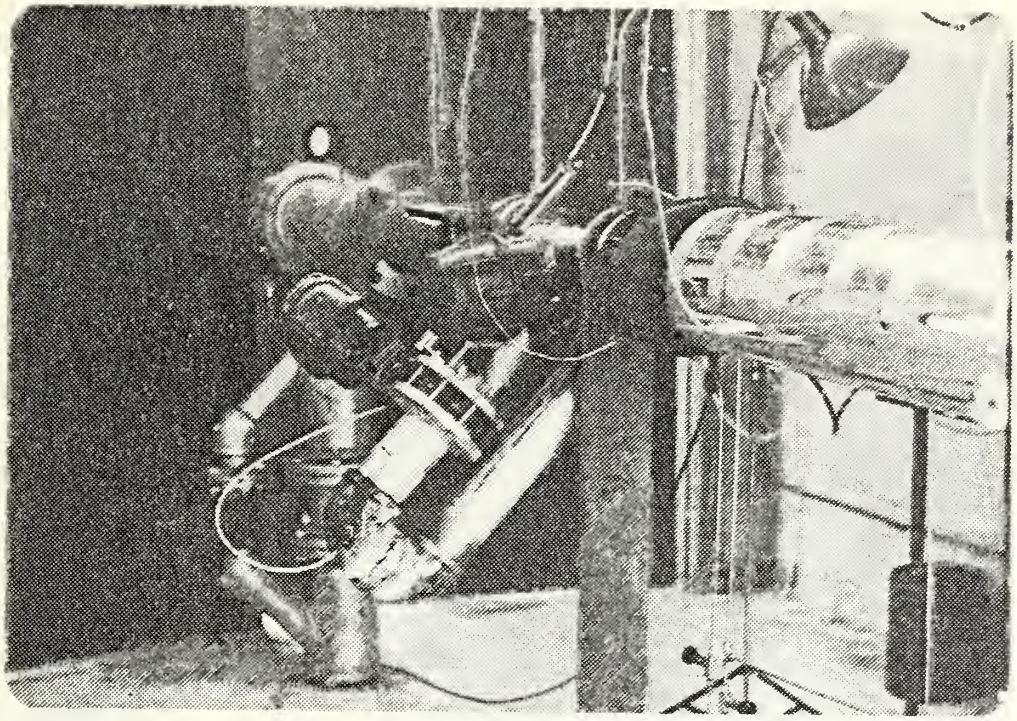

FIGURE 16. Air Supply Piping Arrangement

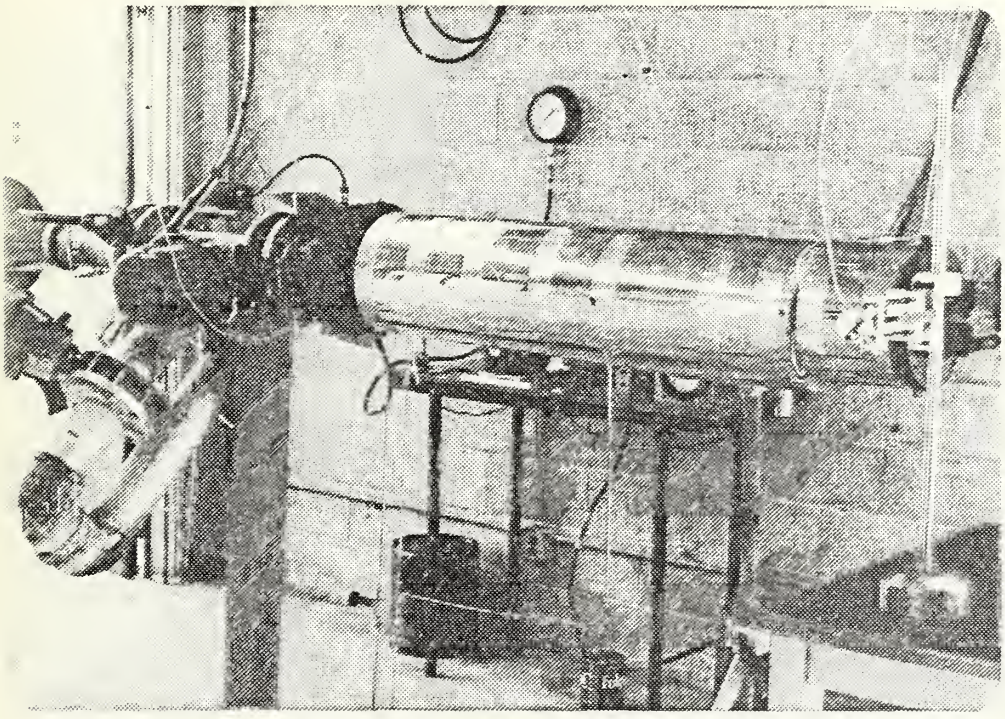

FIGURE 17. Exhaust Stack and Fuel Drains

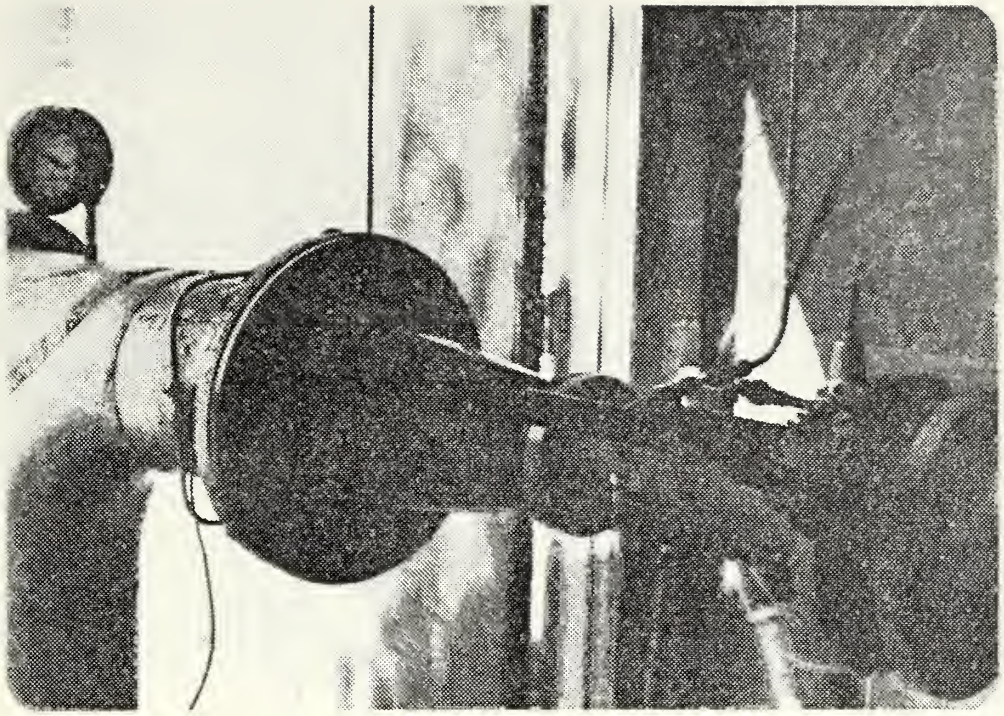

FIGURE 18. Entrance Nozzle and Pressure Taps

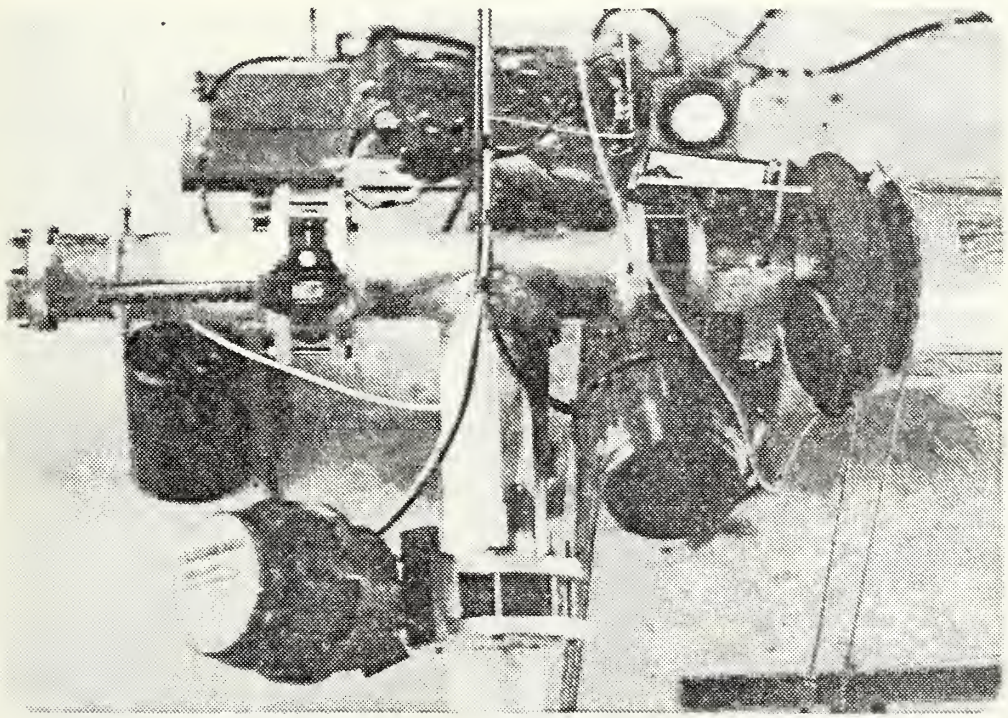

FIGURE 19. Air Splitting Arrangement and Nozzle Box Attachment

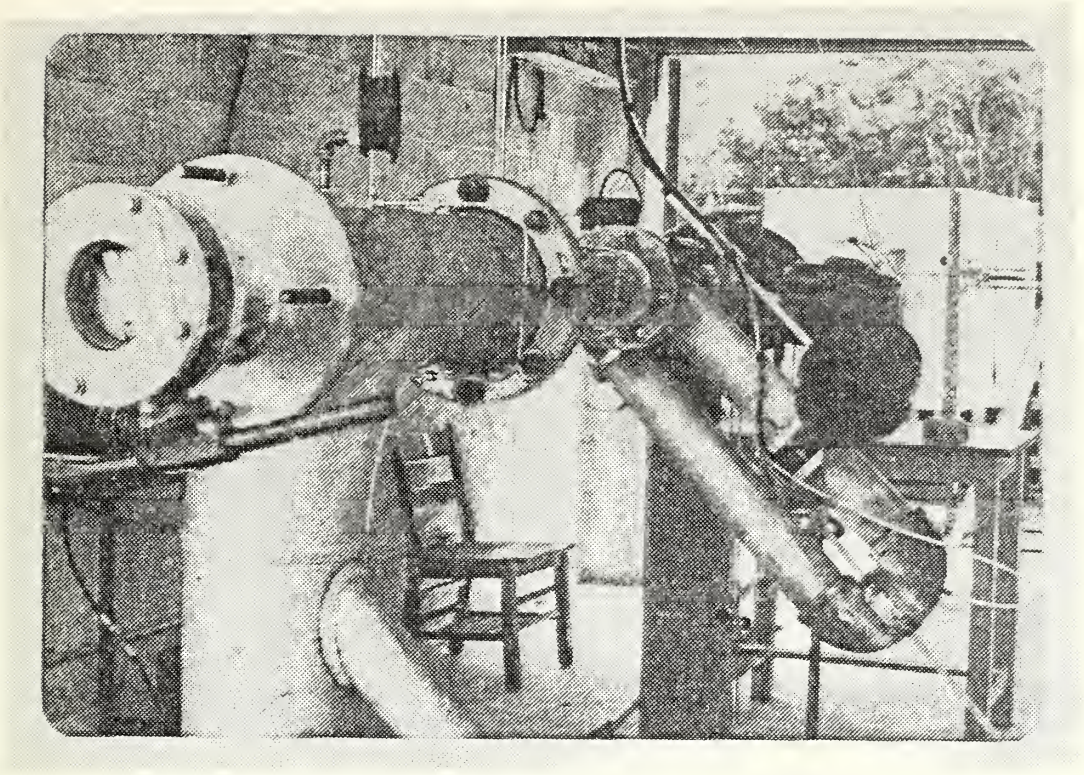

FIGURE 20. Burner Air Supply U-Bend (Right Side)

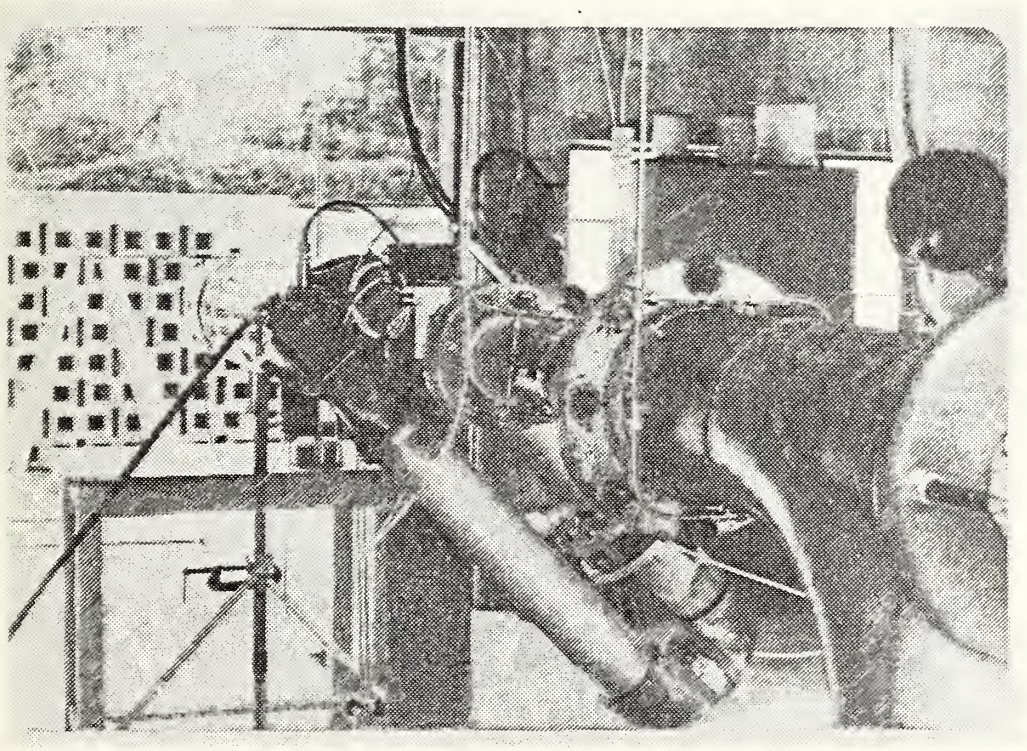

FIGURE 21. Burner Air Supply U-Bend (Left Side)

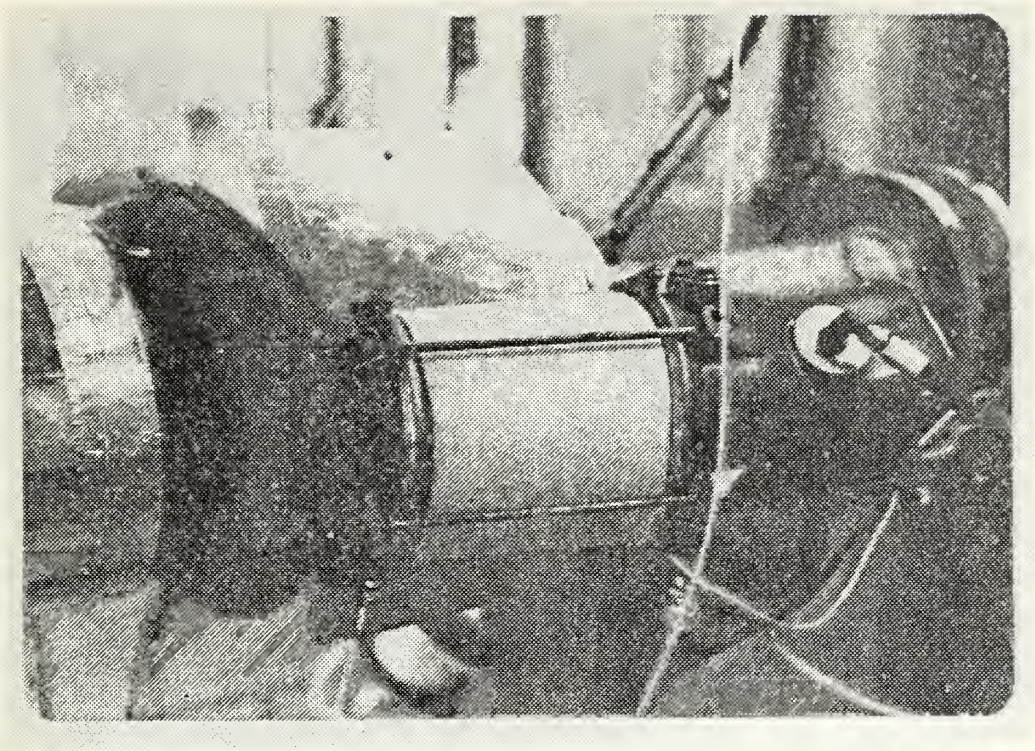

FIGURE 22. Burner Can and Nozzle Box With Heat Shield

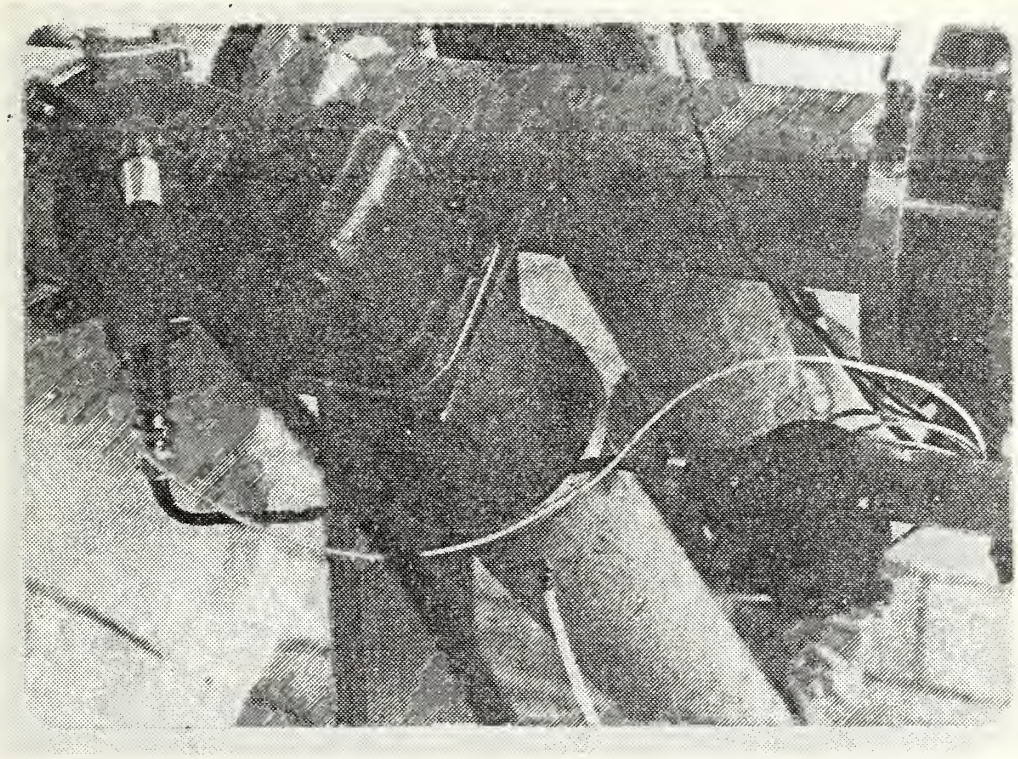

FIGURE 23. Burner Inlet Elbow, Points Set and Ignitor Plug

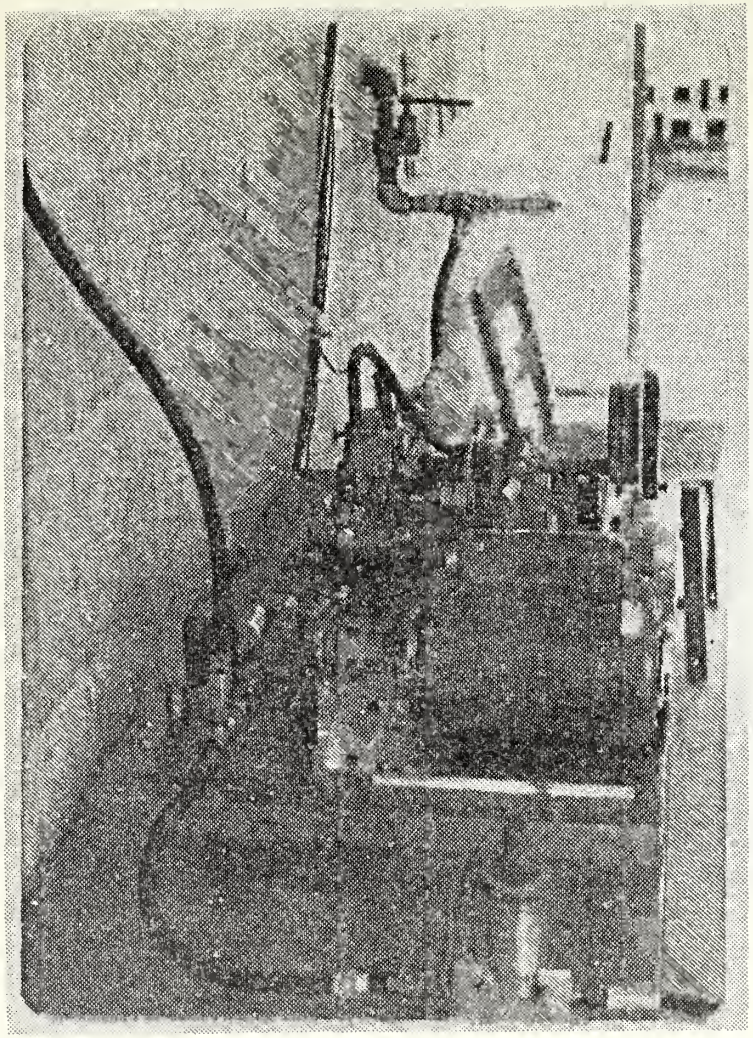

FIGURE 24. Fuel System

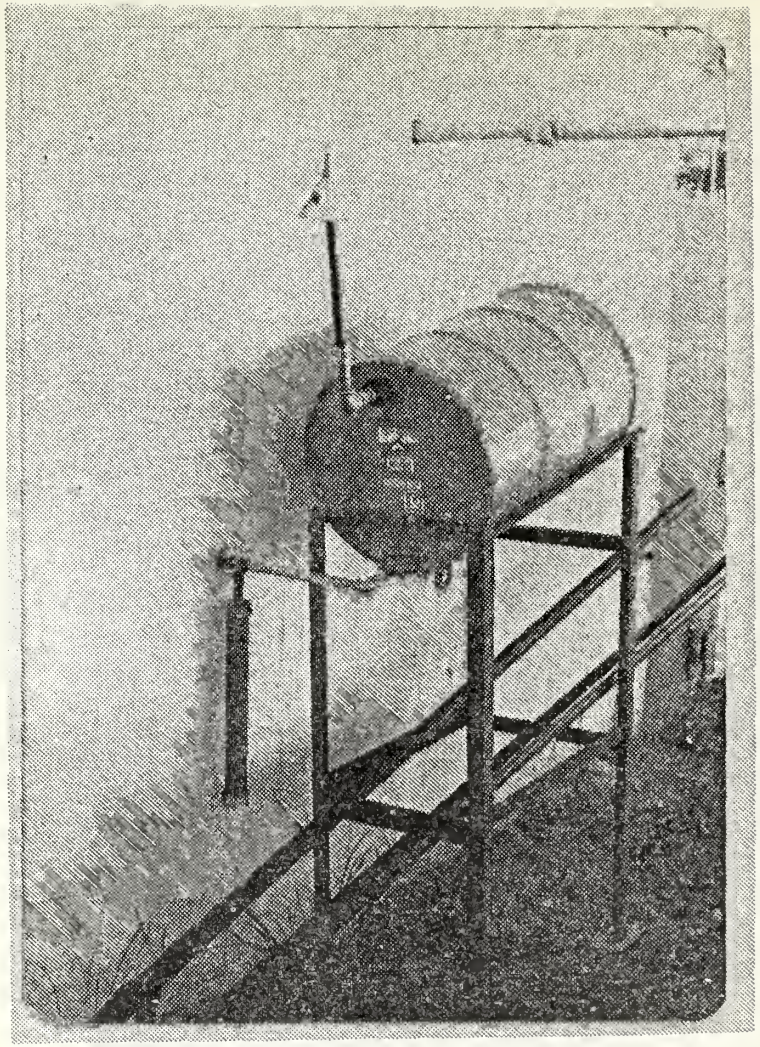

FIGURE 25. Fuel Storage Tank

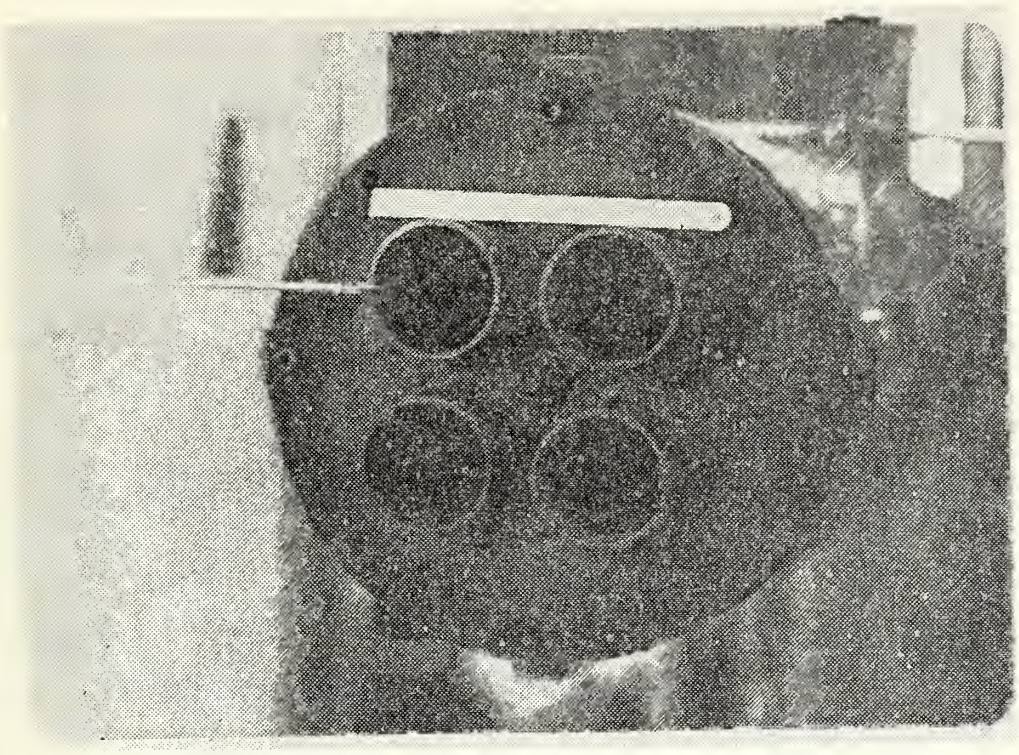

FIGURE 26. Eductor Primary Flow Nozzle Assembly

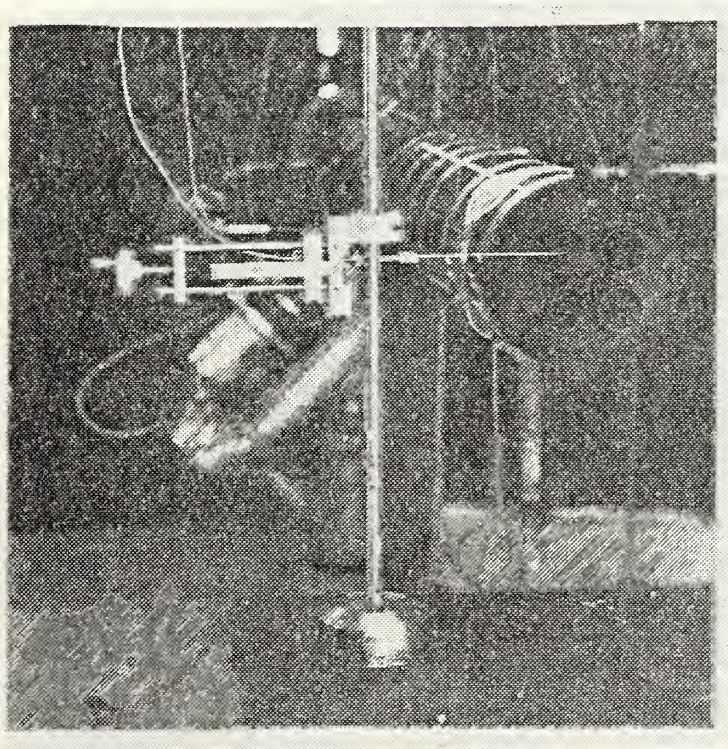

FIGURE 27. Temperature Profile Measuring Apparatus

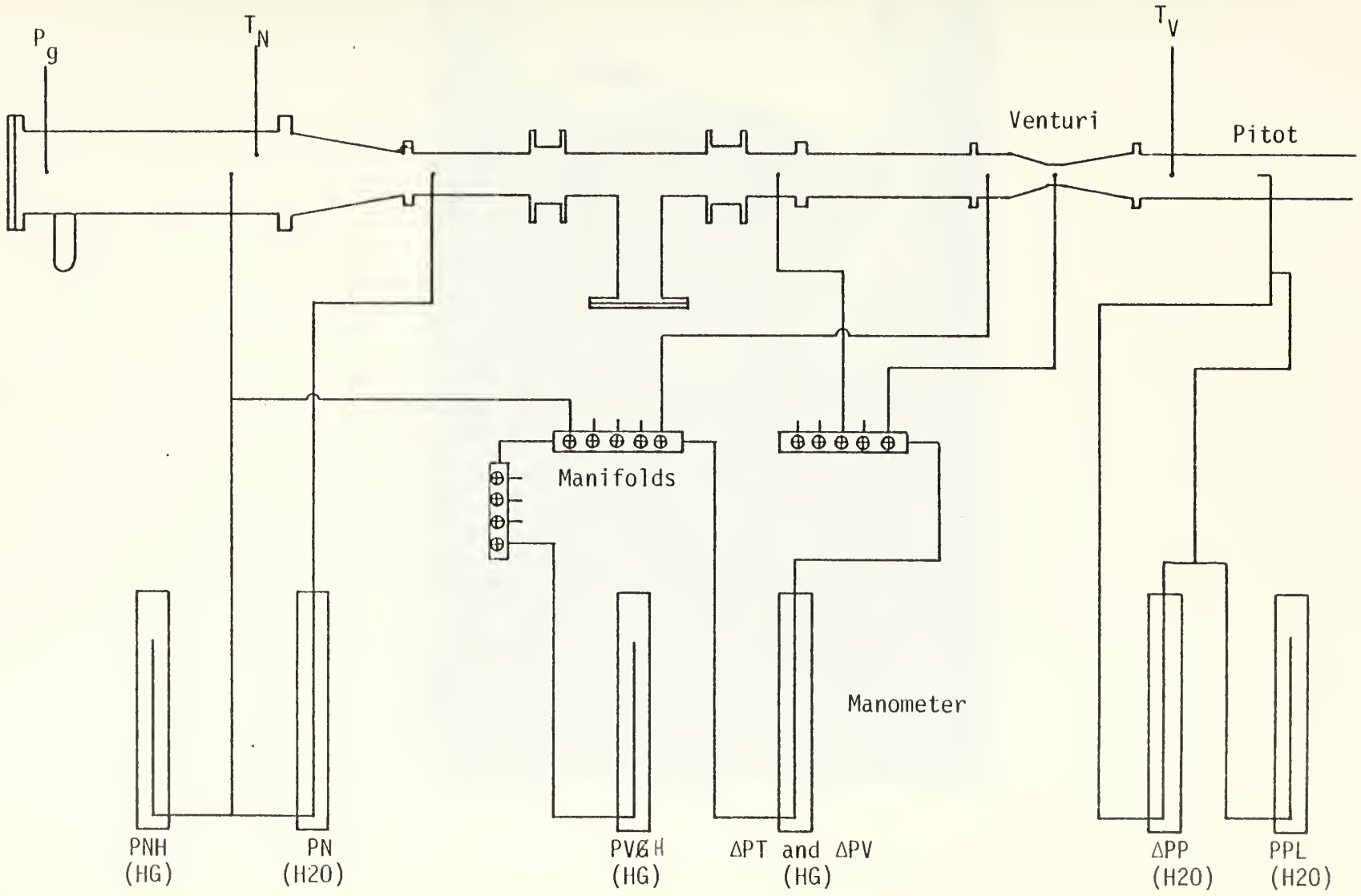

FIGURE 28. Entrance Nozzle Calibration Arrangement

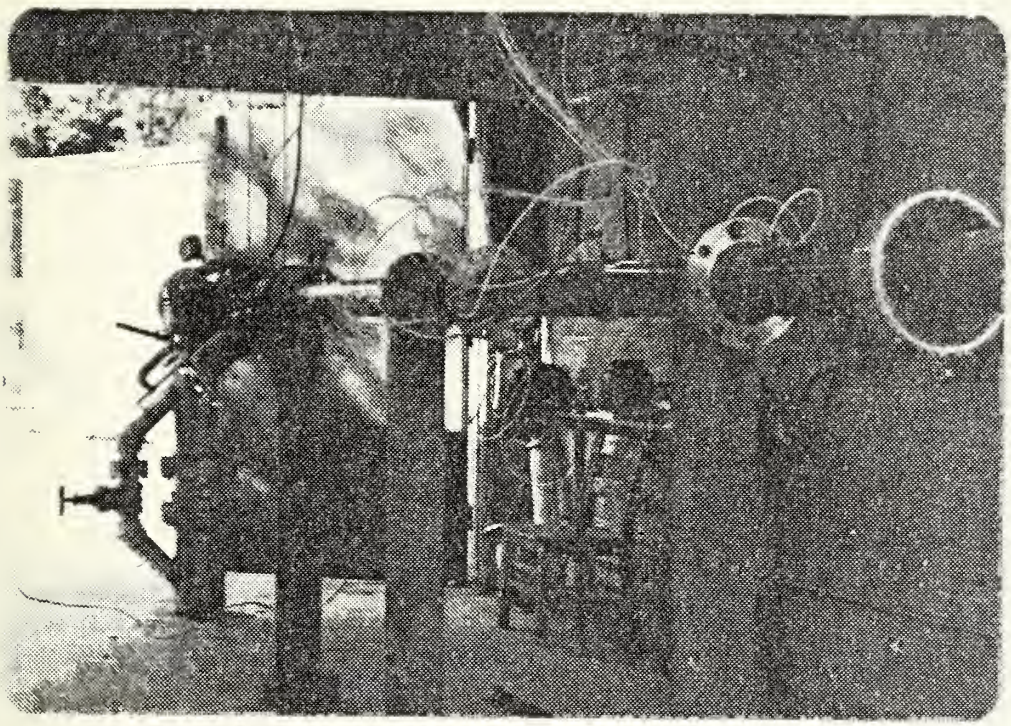

FIGURE 29. Entrance Nozzle Calibration Setup

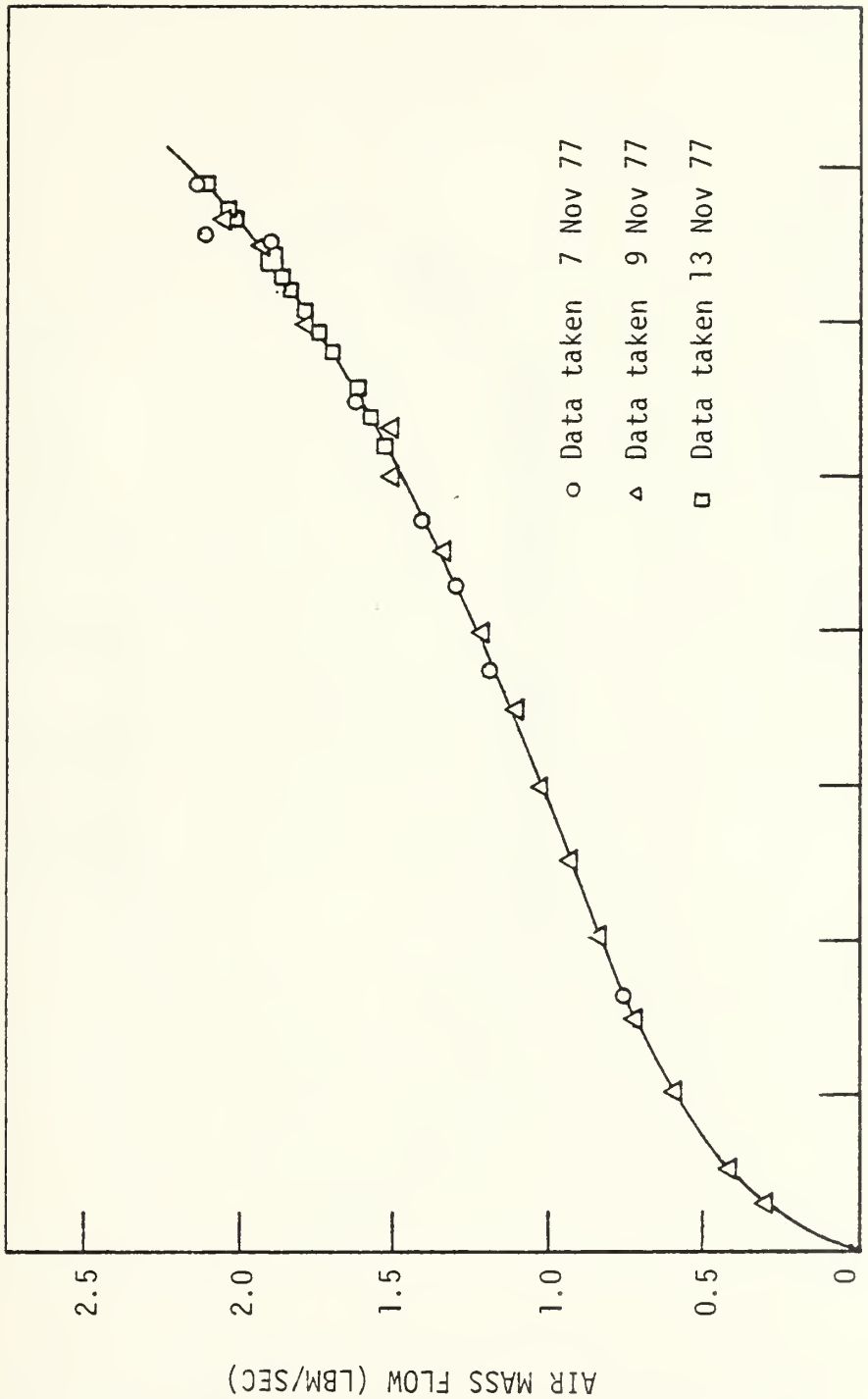

FIGURE 30. Entrance Nozzle Calibration Curve

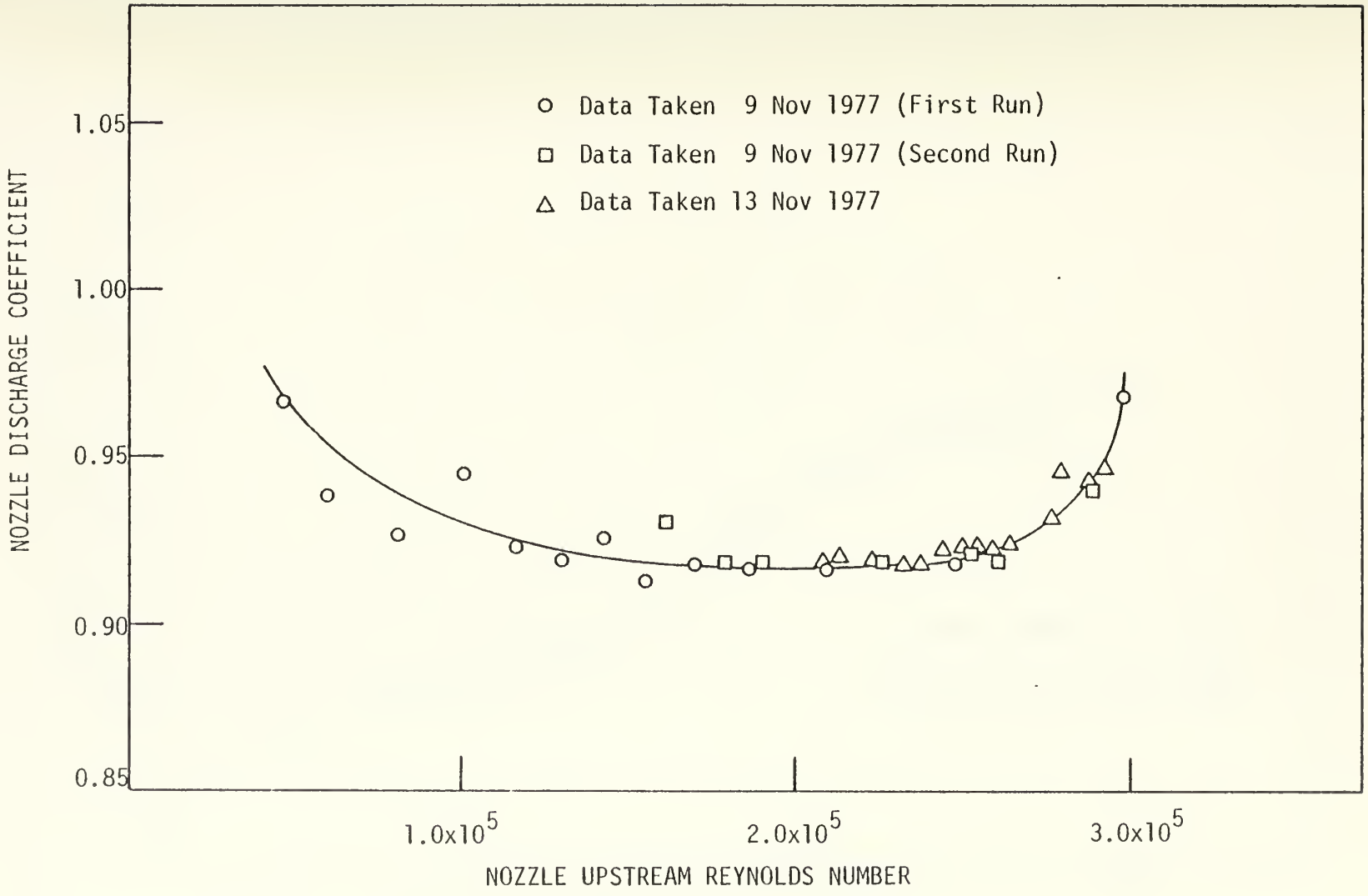

FIGURE 31. Entrance Nozzle Discharge Coefficient Curve

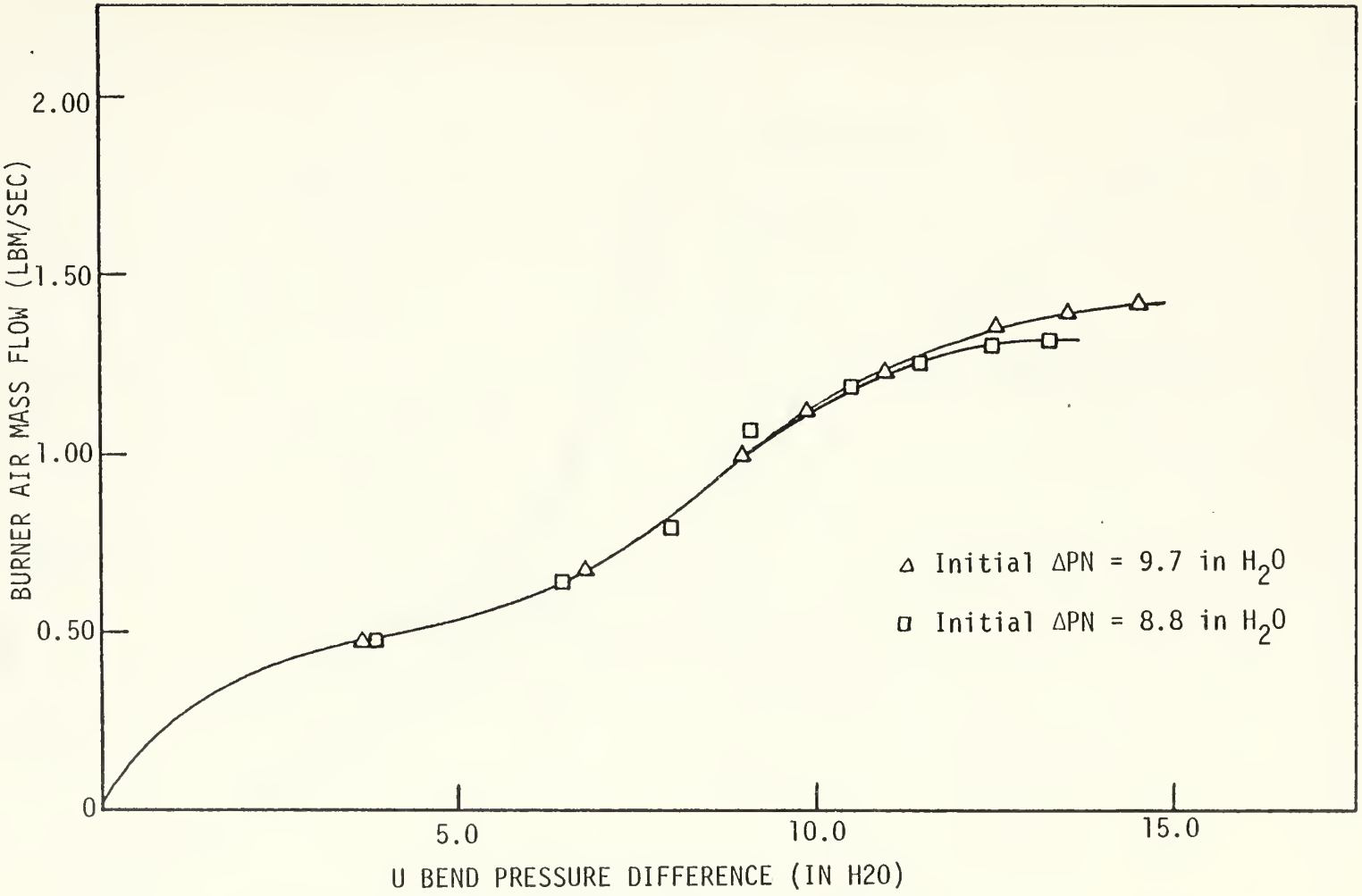

FIGURE 32. U-Bend Mass Flow Calibration Curve

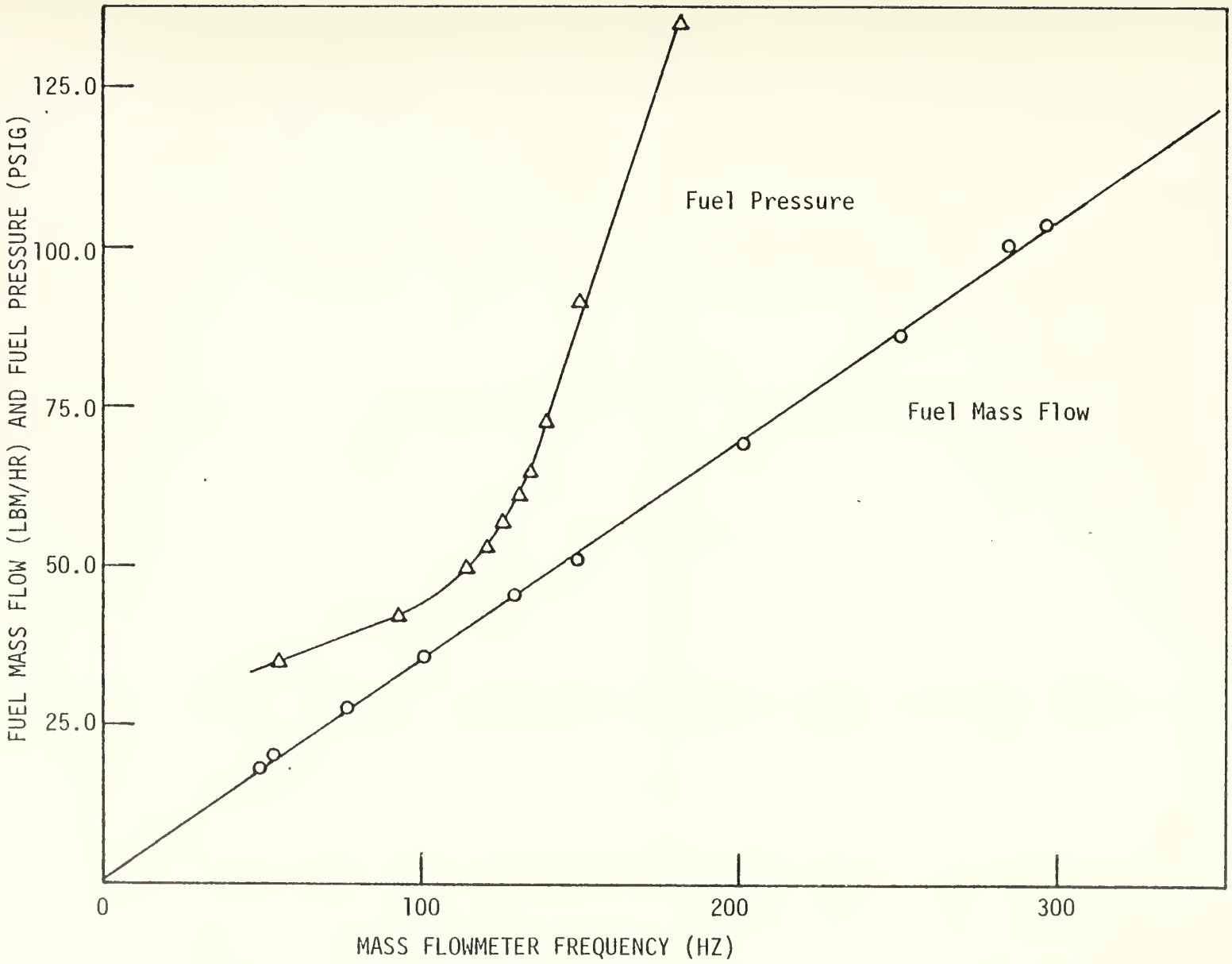

FIGURE 33. Mass Flowmeter Calibration Curve

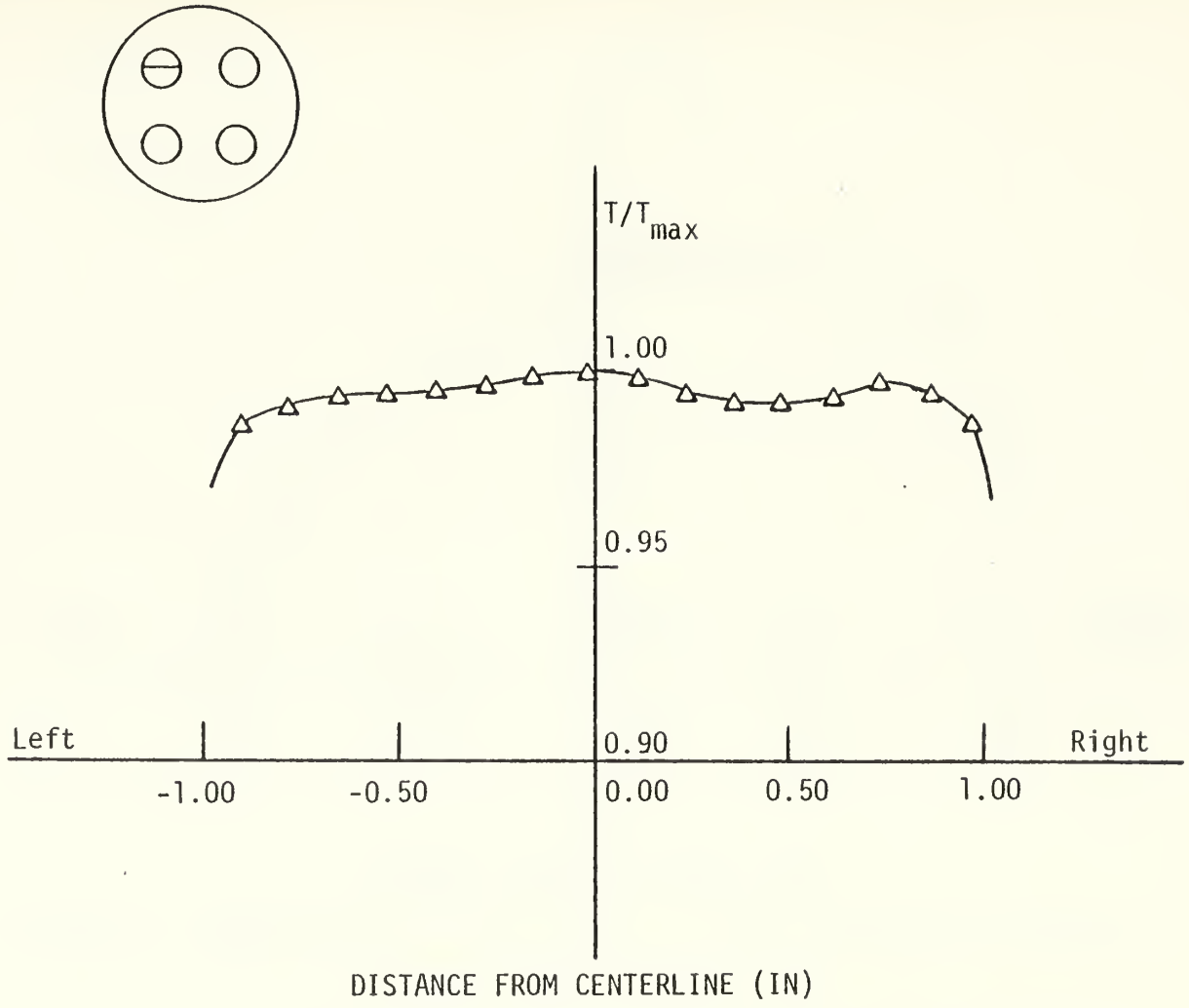

FIGURE 34. Normalized Horizontal Temperature Profile Exhaust Nozzle No. 1

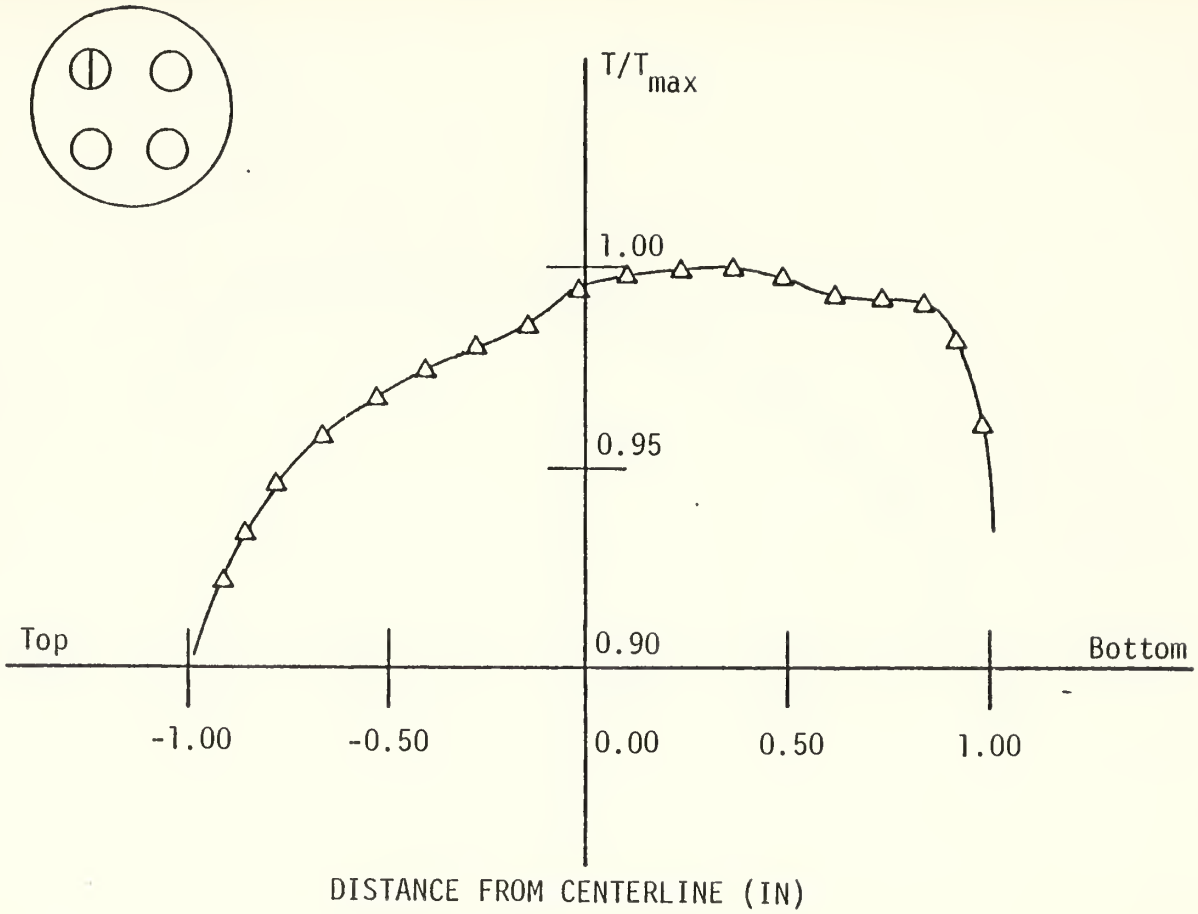

FIGURE 35. Normalized Vertical Temperature Profile Exhaust Nozzle No. 1

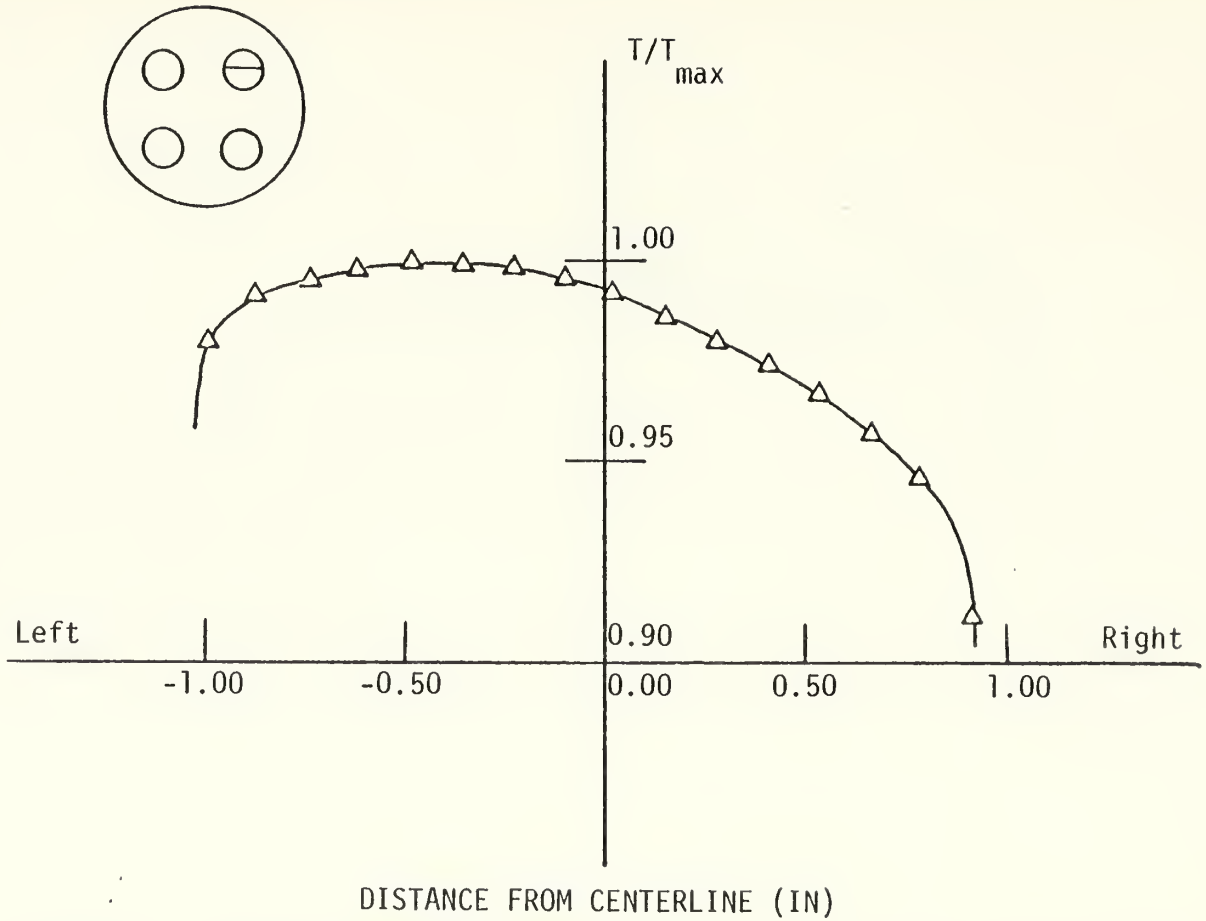

FIGURE 36. Normalized Horizontal Temperature Profile Exhaust Nozzle No. 2

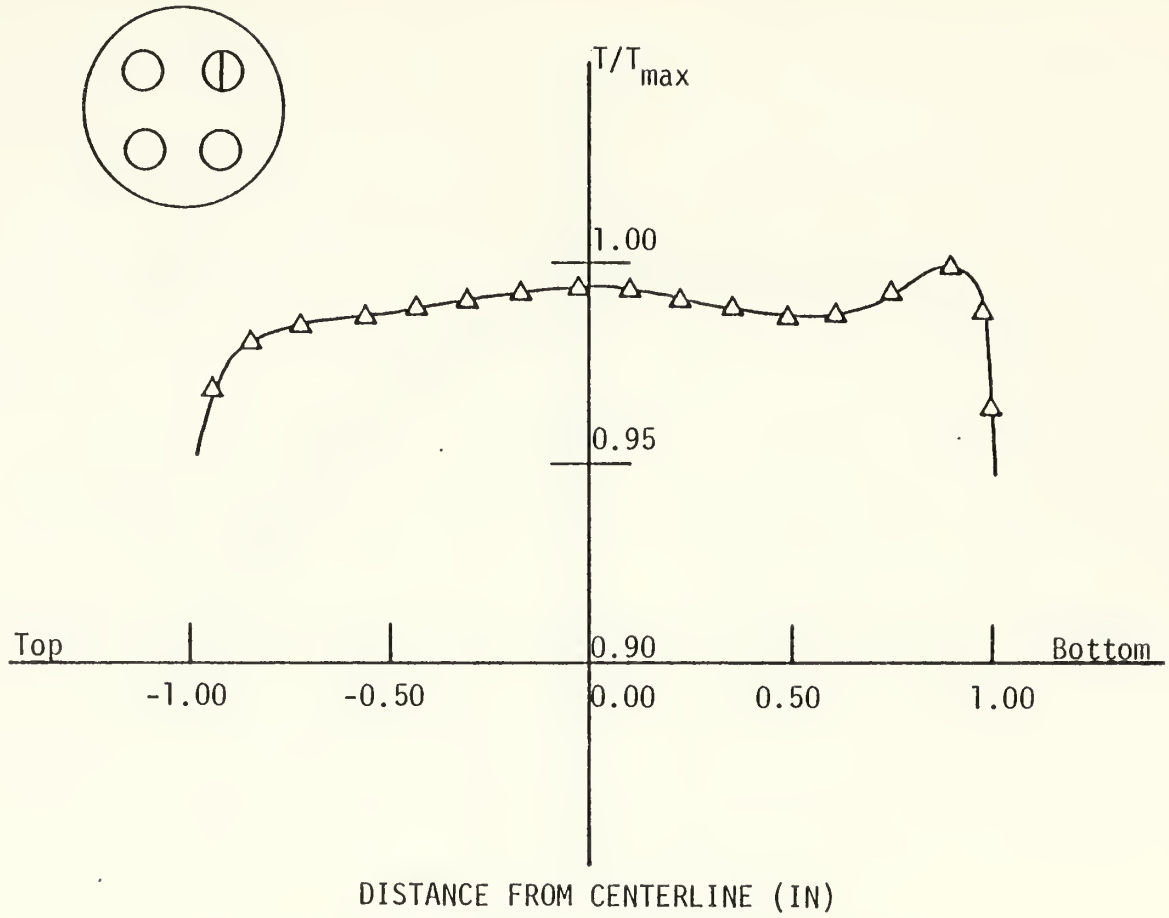

FIGURE 37. Normalized Vertical Temperature Profile Exhaust Nozzle No. 2

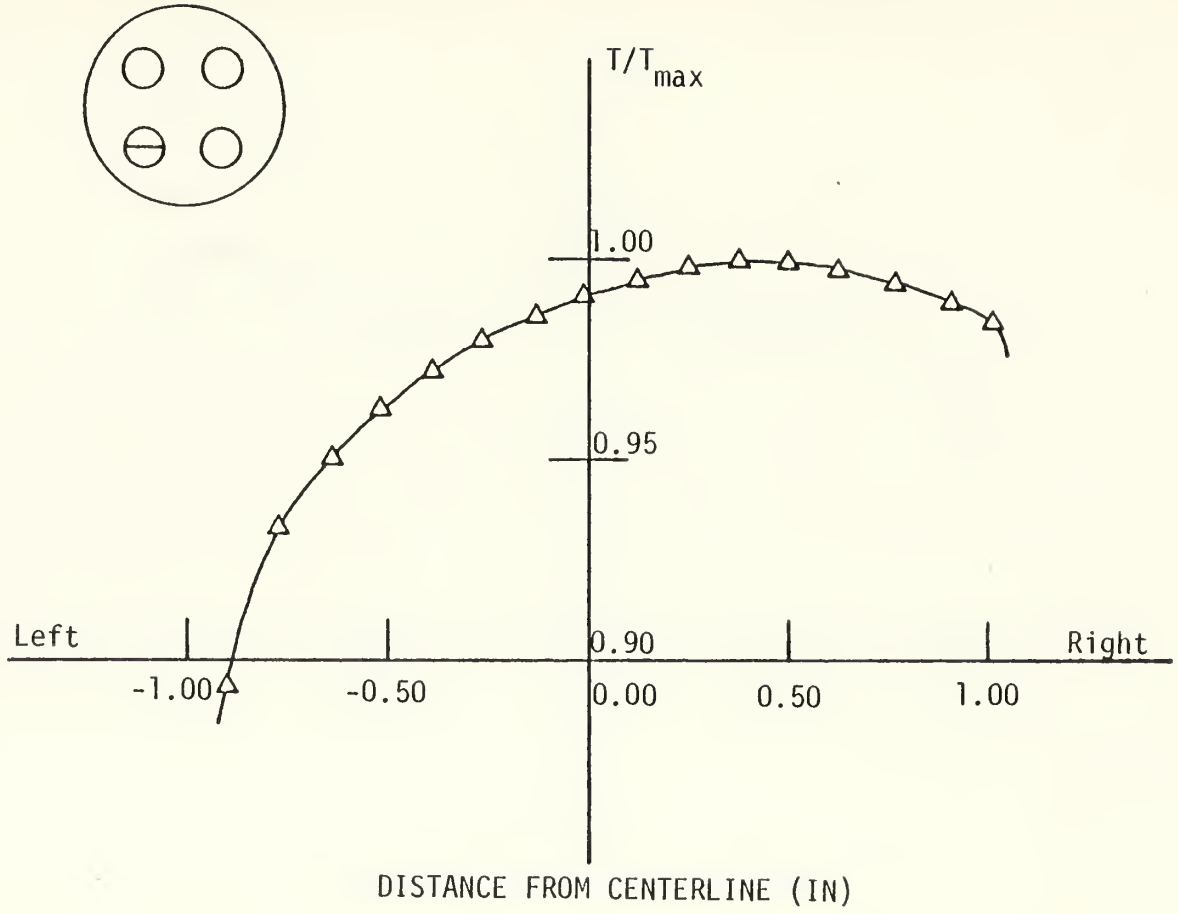

FIGURE 38. Normalized Horizontal Temperature Profile Exhaust Nozzle No. 3

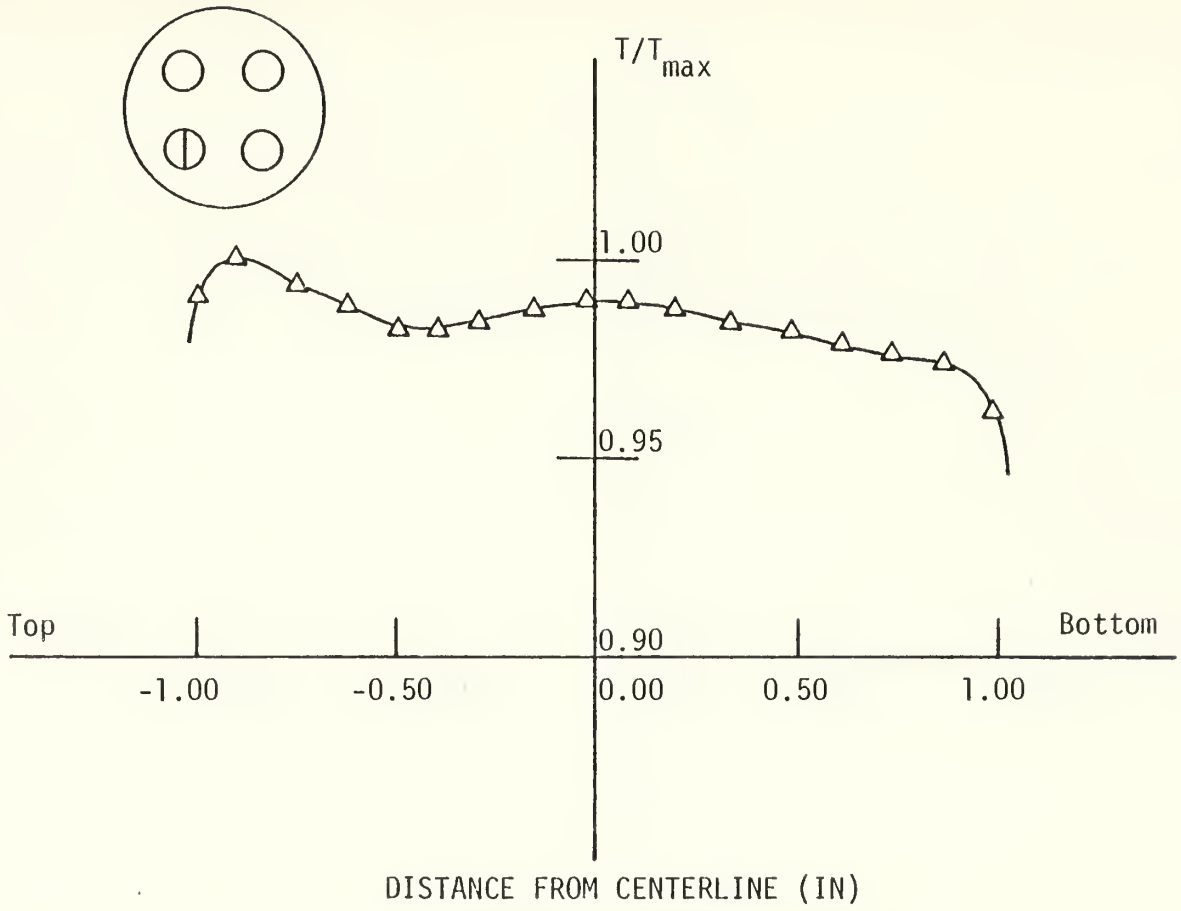

FIGURE 39. Normalized Vertical Temperature Profile Exhaust Nozzle No. 3

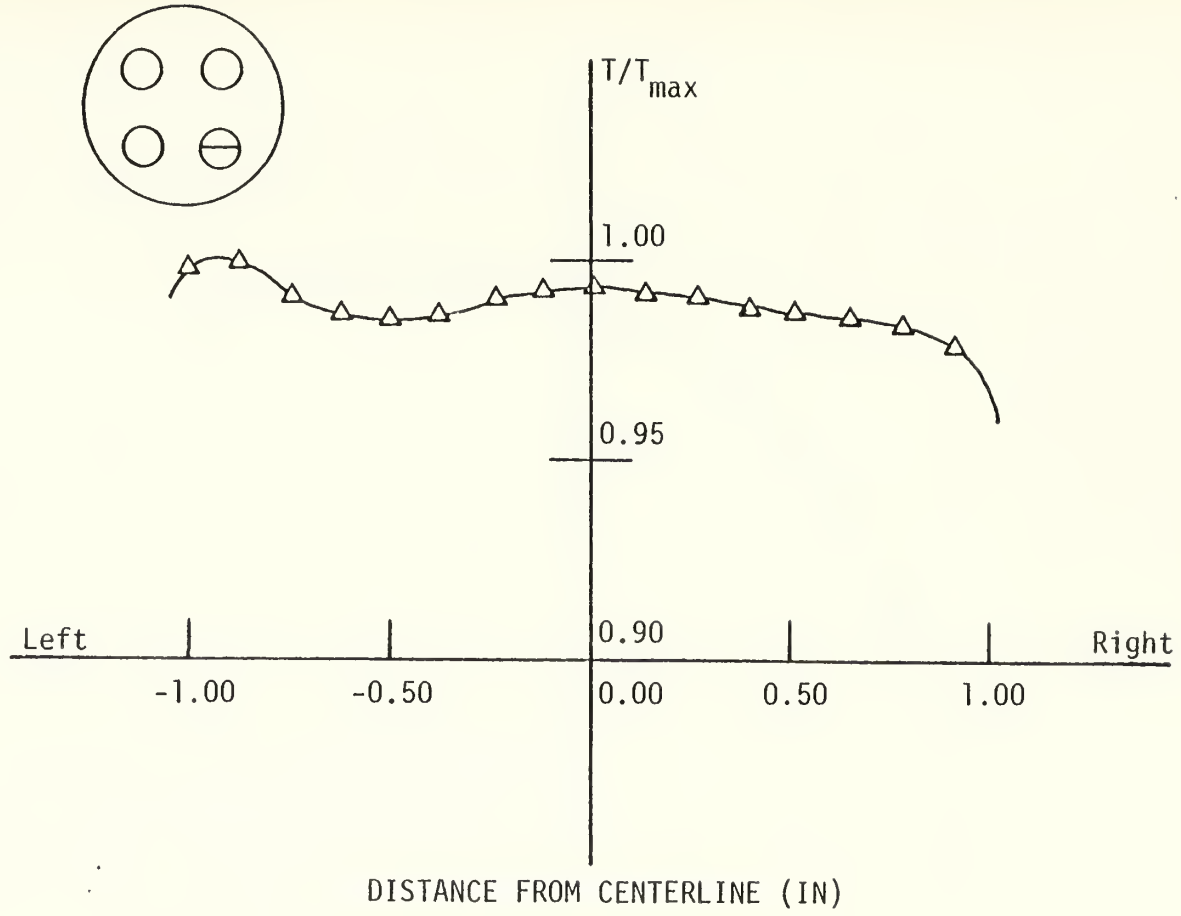

FIGURE 40. Normalized Horizontal Temperature Profile Exhaust Nozzle No. 4

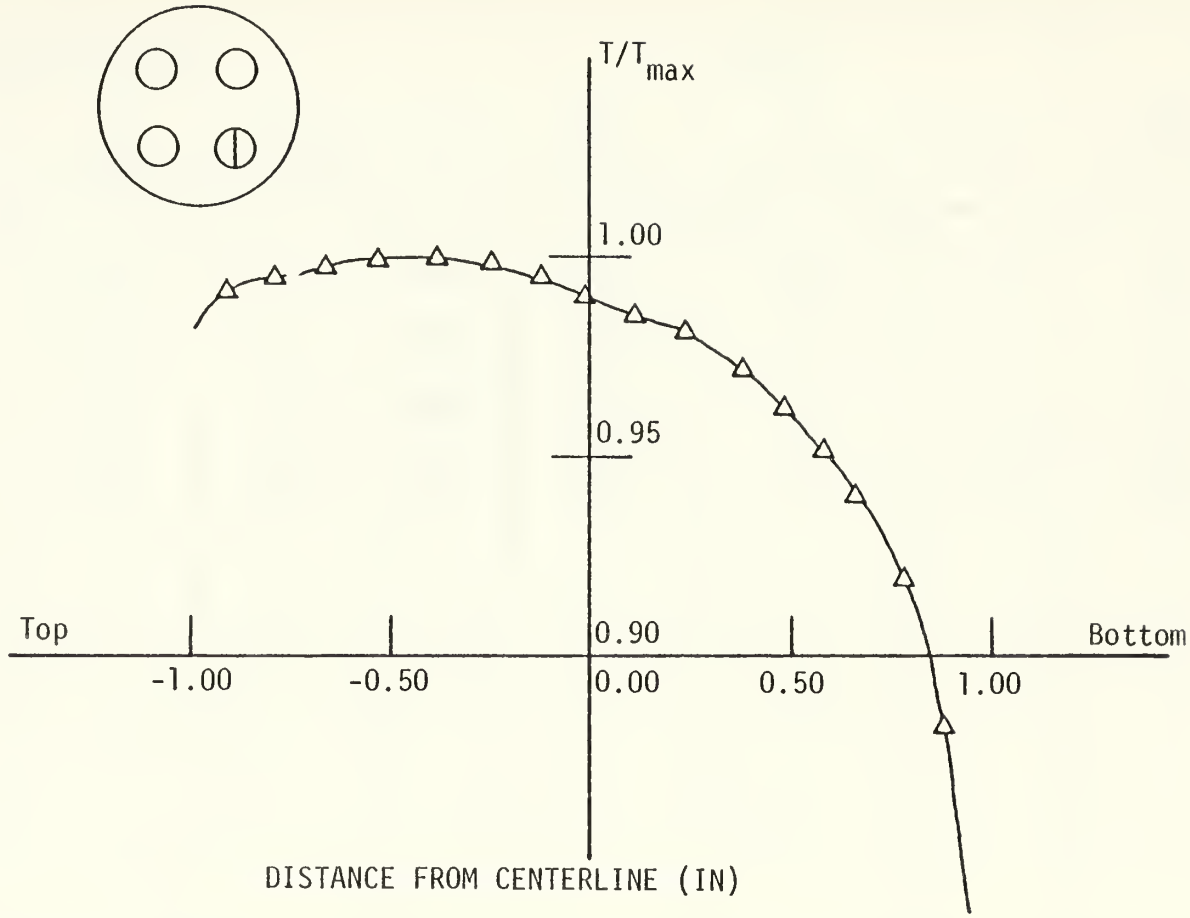

FIGURE 41. Normalized Vertical Temperature Profile Exhaust Nozzle No. 4

Date: 7 November 1977

B = 30.01 in Hg T_a = 62°F

ENTRANCE NOZZLE					VENTURI			PITOT	
P_g (psig)	PNH (in Hg)	ΔPN (in H_2O)	ΔPI (in Hg)	T_N (°F)	PVH (in Hg)	ΔPV (in Hg)	T_V (°F)	PPL (in H_2O)	ΔPP (in H_2O)
14.8	31.35	13.15	3.60	185	28.10	24.40	181	3.90	25.70
6.2	13.65	9.80	2.15	180	11.00	17.20	177	1.95	12.85
1.5	4.00	6.60	1.70	180	2.40	8.70	175	0.95	7.00
0.4	1.55	3.30	0.85	177	0.75	3.50	170	0.45	3.35

TABLE I. Entrance Nozzle Calibration Data Run No. 1

Date: 9 November 1977

B = 30.01 in Hg T_a = 64°F

ENTRANCE NOZZLE					VENTURI			PITOT	
P_g (psig)	PNH (in Hg)	ΔPN (in H_2O)	ΔPT (in Hg)	T_N (°F)	PVH (in Hg)	ΔPV (in Hg)	T_V (°F)	PPL (in H_2O)	ΔPP (in H_2O)
14.5	30.80	13.20	3.55	160	27.55	24.28	155	3.65	25.30
9.9	21.10	12.00	3.15	162	18.15	20.35	161	2.65	17.85
6.0	13.25	10.20	2.65	162	10.80	17.20	161	1.90	12.65
3.9	8.50	9.50	2.35	162	6.35	15.25	161	1.55	10.15
2.4	5.70	8.00	2.05	160	3.75	11.80	160	1.15	8.60
1.8	4.25	7.00	1.80	157	2.10	9.25	158	1.00	7.30
1.4	3.25	6.00	1.55	160	1.85	7.20	155	0.90	6.10
1.0	2.50	5.05	1.25	158	1.35	5.60	153	0.80	5.05
0.6	1.95	4.05	1.02	157	0.95	4.30	152	0.75	4.05
0.4	1.40	3.00	0.75	157	0.65	3.15	152	0.50	3.05
0.2	0.90	2.05	0.55	155	0.40	1.95	149	0.30	2.00
0.0	0.45	1.05	0.30	153	0.20	1.00	146	0.15	1.05
0.0	0.28	0.60	0.18	146	0.10	0.60	140	0.10	0.65
3.4	6.90	8.60	2.20	161	4.85	13.80	157	1.30	9.40
7.9	16.75	11.00	2.85	163	14.10	18.65	158	2.25	14.95
11.0	23.25	12.55	3.30	173	20.25	21.20	165	2.85	19.40
14.6	31.00	13.80	3.65	177	27.75	24.35	173	3.70	25.60
12.0	25.45	13.05	3.40	176	22.30	22.07	172	3.00	21.00
2.1	5.00	7.58	1.95	173	3.20	10.65	162	1.10	8.05
4.5	10.15	9.45	2.45	175	7.85	16.00	168	1.75	10.95

TABLE II. Entrance Nozzle Calibration Data Run No. 2

Date: 13 November 1977

B = 30.95 in Hg T_a = 61°F

ENTRANCE NOZZLE					VENTURI			PITOT	
P_g (psig)	PNH (in Hg)	ΔPN (in H_2O)	ΔPT (in Hg)	T_N (°F)	PVH (in Hg)	ΔPV (in Hg)	T_V (°F)	PPL (in H_2O)	ΔPP (in H_2O)
14.6	31.10	13.80	3.65	181	27.80	24.40	176	3.90	25.55
14.6	31.00	13.80	3.63	172	27.75	24.40	160	3.85	25.40
14.0	29.50	13.35	3.55	180	26.30	23.80	175	3.70	24.25
13.2	27.70	13.37	3.52	172	24.45	23.02	161	3.40	22.80
12.0	25.35	13.05	3.45	173	22.25	22.05	163	3.05	21.00
11.5	24.45	12.85	3.37	175	21.40	21.70	164	3.00	20.35
11.0	23.40	12.60	3.30	175	20.40	21.30	166	2.95	19.55
10.5	22.60	12.45	3.25	175	19.65	21.00	165	2.87	19.10
10.0	21.30	12.15	3.15	175	18.40	20.45	165	2.70	18.05
9.5	20.10	11.90	3.10	177	17.25	20.00	171	2.60	17.30
9.0	19.10	11.65	3.03	177	16.35	19.60	172	2.50	16.60
8.0	17.20	11.15	2.90	177	14.55	18.80	172	2.30	15.25
7.0	15.10	10.65	2.97	177	12.55	18.00	172	2.15	13.90
6.5	13.95	10.40	2.70	177	11.45	17.55	172	2.10	13.15

TABLE III. Entrance Nozzle Calibration Data Run No. 3

ΔPN (in H_2O)	$\dot{m}_a$ (lbm/sec)
31.35	2.117
31.10	2.118
31.00	2.119
30.80	2.141
29.50	2.063
27.70	2.019
25.45	1.915
25.35	1.933
24.45	1.899
23.40	1.862
23.25	1.850
22.60	1.835
21.30	1.789
21.10	1.786
20.10	1.740
19.10	1.703
17.20	1.636
16.75	1.632
15.10	1.566
13.95	1.524
13.65	1.496
13.25	1.511
10.15	1.394
8.50	1.342
6.90	1.288
5.70	1.218
5.00	1.179
4.25	1.112
4.00	1.115
3.25	1.030
2.50	0.933
1.95	0.834
1.55	0.753
1.40	0.725
0.90	0.584
0.45	0.424
0.28	0.330

TABLE IV. Entrance Nozzle Calibration

Re_{DN} ($x10^{-5}$)	C_{dN}
2.972	0.9675
2.929	0.9470
2.883	0.9406
2.868	0.9427
0.796	0.9452
2.762	0.9329
2.642	0.9241
2.607	0.9189
2.589	0.9238
2.539	0.9237
2.528	0.9214
2.502	0.9227
2.472	0.9178
2.439	0.9221
2.367	0.9185
2.316	0.9177
2.257	0.9193
2.225	0.9190
2.130	0.9208
2.091	0.9169
2.073	0.9186
1.900	0.9198
1.857	0.9158
1.785	0.9185
1.691	0.9178
1.611	0.9310
1.549	0.9132
1.430	0.9254
1.298	0.9192
1.162	0.9230
1.010	0.9448
0.815	0.9264
0.593	0.9385
0.466	0.9657

TABLE V. Entrance Nozzle Discharge Coefficient

Date: 24 November 1977

B = 30.13 in Hg T_a = 62°F Bypass Air Valve Closed

ΔPN (in H_2O)	PNH (in Hg)	ΔPU (in H_2O)	PUH (in Hg)	T_N (°F)	T_B (°F)	Burner Supply Valve Position (% open)
RUN 1	Initial ΔPN = 8.8 in H_2O					
8.80	10.20	13.25	7.95	150.8	145	100
8.70	10.50	12.50	7.85	151.9	146	70
8.30	11.45	11.45	7.60	152.6	147	65
7.70	12.85	10.50	7.35	154.0	148	58
6.45	16.30	9.10	6.60	154.4	149	52
3.55	24.60	8.00	4.60	153.4	147	40
2.50	27.90	6.50	3.55	152.4	146	30
1.30	31.85	3.40	2.05	158.5	145	20
RUN 2	Initial ΔPN = 9.7 in H_2O					
9.70	11.40	14.60	8.90	169.7	151	100
9.50	11.85	13.60	8.70	159.1	153	80
9.10	12.75	12.60	8.50	160.3	154	65
8.05	15.00	11.00	7.95	160.9	155	55
7.10	17.20	9.90	7.35	161.6	156	50
5.70	24.45	9.00	5.30	160.8	155	40
2.60	28.80	6.80	3.70	159.3	154	30
1.30	32.40	3.70	2.10	157.0	151	20

TABLE VI. U-Bend Calibration Data

ΔPU (in H_2O)	$\dot{m}_a$ (lbm/sec)
RUN 1	
13.25	1.32
12.50	1.30
11.45	1.25
10.50	1.18
9.10	1.07
8.00	0.78
6.50	0.65
3.40	0.47
RUN 2	
14.60	1.43
13.60	1.40
12.60	1.36
11.00	1.22
9.90	1.12
9.00	1.00
6.80	0.67
3.70	0.47

TABLE VII. U-Bend Calibration

Date: 21 November 1977

T_f = 61.2°F

T_a = 62.2°F

FREQUENCY (Hz)	TIME (Sec)	FUEL WEIGHT (Lb)
285.0	17.99	0.5
468.0	10.99	0.5
297.5	34.59	1.0
202.0	52.12	1.0
54.0	84.83	0.5
101.0	98.66	1.0
251.5	41.54	1.0
150.0	68.42	1.0
77.5	63.30	0.5
130.0	71.18	0.9

TABLE VIII. Mass Flowmeter Calibration Data

FREQUENCY (Hz)	$\dot{m}_f$ (lbm/hr)
285.0	100.06
468.0	163.79
297.5	104.08
202.0	69.07
54.0	21.22
101.0	36.49
251.5	86.66
150.0	52.62
77.5	28.44
130.0	45.52

TABLE IX. Mass Flowmeter Calibration

Date: 30 November 1977

B = 30.02 in Hg T_a = 63°F

	START	POINT 1	POINT 2	POINT 3	POINT 4	POINT 5
PNH (in Hg)*		7.35	6.75	6.75	6.37	5.97
ΔPN (in H_2O)		8.42	8.51	8.64	8.72	8.82
ΔPT (in Hg)		6.65	6.02	6.05	5.67	5.28
PUH (in Hg)		5.88	5.25	5.27	6.37	4.50
ΔPU (in H_2O)*	1.00	4.80	4.25	4.30	3.92	3.65
PEH (in Hg)		1.88	1.73	1.72	1.64	1.55
P_g (psig)		3.20	3.00	3.00	2.70	2.40
T_N (°F)*		173.6	171.3	169.3	164.7	156.9
T_B (°F)		1173	1203	1176	1192	1200
T_{BB} (°F)		1148	1172	1148	1157	1159
T_{SV} (°F)		861	825	802	786	756
T_{SH} (°F)		862	829	806	780	756
T_{e1} (°F)		850	828	800	782	755
T_{e2} (°F)		848	824	800	779	748
T_{e3} (°F)		850	825	803	779	755
T_{e4} (°F)		853	826	805	782	761
T_F (°F)		58.2	58.2	57.8	57.8	57.3
T_R (°F)		95.9	95.8	95.0	94.7	94.6
f (Hz)	113	140.0	135.0	131.0	126.0	122.0
P_F (psig)*	55.0	73.0	65.0	62.0	57.0	53.0
P_S (psig)	14.0	14.0	14.0	14.0	14.0	14.0
V_S (% open)	100	100	100	100	100	100
V_B (% open)*	100	30	32	32	35	40

*Indicates Critical Operating Point Parameter

TABLE X. Operating Point Data

AIR MASS FLOW (lb/sec)	FUEL MASS FLOW (lb/hr)	EXHAUST TEMPERATURE (°F)	OVERALL AFR	M
1.262	49.5	850	91	0.081
1.262	48.0	825	95	0.080
1.277	46.8	802	98	0.080
1.276	44.0	780	105	0.080
1.285	43.0	755	108	0.080

TABLE XI. Operating Point Summary

*Indicates T_{max}

Distance (in)	Horizontal Temperature (°F)	Vertical Temperature (°F)
0.125	844	801
0.250	847	823
0.375	850	833
0.500	850	841
0.625	851	847
0.750	852	852
0.875	854	857
1.000	855*	865
1.125	853	865
1.250	850	867
1.375	848	869*
1.500	848	867
1.625	850	863
1.750	853	863
1.875	850	860
2.000	845	836

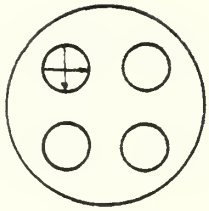

Coordinate System

TABLE XII. Exhaust Nozzle No. 1 Temperature Profile Data

*Indicates T_{max}

Distance (in)	Horizontal Temperature (°F)	Vertical Temperature (°F)
0.125	788	848
0.250	818	854
0.375	828	856
0.500	836	858
0.625	842	859
0.750	847	860
0.875	852	862
1.000	857	863
1.125	861	862
1.250	863	860
1.375	863	858
1.500	864*	857
1.625	862	858
1.750	860	862
1.875	856	868*
2.000	847	838

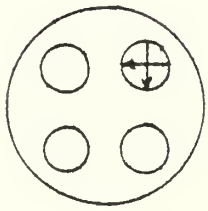

Coordinate System

TABLE XIII. Exhaust Nozzle No. 2 Temperature Profile Data

*Indicates T_{max}

Distance (in)	Horizontal Temperature (°F)	Vertical Temperature (°F)
0.125	770	873*
0.250	804	868
0.375	820	864
0.500	830	858
0.625	838	858
0.750	845	861
0.875	850	862
1.000	855	864
1.125	858	863
1.250	860	862
1.375	862*	859
1.500	862	859
1.625	860	855
1.750	857	853
1.875	854	851
2.000	850	840

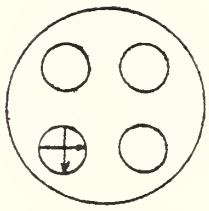

Coordinate System

TABLE XIV. Exhaust Nozzle No. 3 Temperature Profile Data

*Indicates T_{max}

Distance (in)	Horizontal Temperature (°F)	Vertical Temperature (°F)
0.125	850	860
0.250	854	862
0.375	856	865
0.500	857	867*
0.625	858	867
0.750	860	865
0.875	861	863
1.000	862	858
1.125	861	854
1.250	859	851
1.375	857	842
1.500	856	833
1.625	857	820
1.750	860	800
1.875	868*	764
2.000	867	633

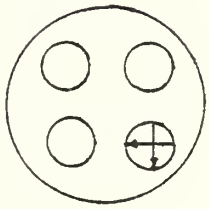

Coordinate System

TABLE XV. Exhaust Nozzle No. 4 Temperature Profile Data

APPENDIX A

CALCULATION OF ENTRANCE NOZZLE MASS FLOW AND DISCHARGE COEFFICIENT

For the classic Herschel Venturi tube the calculation of mass flow rate is given by [13]:

$$\dot{m} = 0.099702 C_d Y d^2 F (1-\beta^4)^{-0.5} (\rho h_W / RT)^{0.5} \qquad (a)$$

The symbols and units applying to the above equation are:

C_d	coefficient of discharge	ratio
d	Venturi throat diameter	inches (2.130)
F	Area thermal-expansion factor	dimensionless
h_W	Differential pressure	inches of $H_2 0$
$\dot{m}$	Mass rate of flow	lbm/sec
ρ	Pressure	psfa
R	Gas constant for air	ft-lbf/lbm-°R
Y	Expansion factor	ratio
T	Temperature	°R
β	Diameter ratio	ratio (0.5)

In terms of the symbology used in this report, P = PVH + B, $T = T_v$ and $h_W = \Delta PV$, or

$$\dot{m}_a = 0.99702 C_d Y d^2 F (1-\beta^4)^{-0.5} [(\rho VH+\beta)\Delta PV/RT_v]^{0.5}$$

maintaining consistent units. For the first line of data in Table 2, PVH = 27.55 in Hg, β = 30.01 in Hg, T_v = 155°F and PV = 24.28 in Hg. The values of Y and F can be found from tables in Reference 13 to be Y = 0.7280 and F = 1.0018. A value of C_d must be chosen from the calibration curve provided for the Venturi [14]. In this case C_d = 0.9840. After conversion to appropriate units the above data results in an $\dot{m}_a$ of 2.141 lbm/sec. From the mass flow rate the Reynolds number can be determined.

$$Re_D = \frac{48\ \dot{m}_a}{\pi D \mu}$$

where D is the inlet diameter (inches) and μ is the upstream absolute viscosity of the fluid (lbm/ft-sec). In this case $Re_D = 5.614 \times 10^5$. Using this Reynolds number the Venturi calibration curve is entered and the corresponding C_d is checked against that chosen for the calculation of $\dot{m}_a$. If the two coefficients agree, as they do in this case, $\dot{m}_a$ is valid. If the coefficients do not agree a new C_d is chosen based upon Re_D and the process is repeated. The resulting mass flow rate then correlates with a measured ΔPN at the entrance nozzle for the given conditions.

Since the mass flow rate just determined is strictly valid only for the measured temperature and pressure at

that data point, it is necessary to nondimensionalize the data in terms of an entrance nozzle discharge coefficient (C_{DN}) which can be used for varying temperatures and pressures. Rearranging equation (a) gives

$$C_{DN} = \frac{\dot{m}_a (1-\beta_N{}^4)^{0.5} (\rho h_W/RT)^{-0.5}}{0.099702\ Y\ d^2\ F} \quad .$$

Now the parameters are evaluated at the entrance nozzle. F was assumed equal to 1.0. The ratio of the diameters (β_N) for the entrance nozzle was 0.510. In terms of the symbology used in this report,

$$C_{DN} = \frac{\dot{m}_a (1-\beta_N{}^4)^{0.5} [(PNH+B)\,\Delta PN/RT_N]^{-0.5}}{0.099702\ Y\ d_N{}^2} \quad .$$

Using the first line of data in Table (2) PNH = 30.80 in Hg, ΔPN = 13.20 in H_2O, T_N = 160°F and d_N = 4.080 inches. C_{DN} is evaluated to be 0.9675. The Reynolds number based upon the nozzle inlet diameter can now be calculated and C_{DN} plotted as a function of Re_{DN} (Figure 31).

APPENDIX B

OPERATING POINT MASS FLOW CALCULATIONS

To determine the mass flow rates at a given operating point $\dot{m}_a$ is calculated using the entrance nozzle discharge coefficient as follows:

$$\dot{m}_a = 0.099702 C_{DN} Y d_N^2 (1-\beta^4)^{-0.5} [(PNH+\mathbf{B})\Delta PN/RT_N]^{0.5}$$

where d_N is in inches, PNH and $\mathbf{B}$ are in psfa, ΔPN is in inches of H_20 and T_N is in °R. Y may be determined from Reference 13. Since $\dot{m}_f$ is a measured quantity,

$$AFR = \dot{m}_a/\dot{m}_f .$$

The exhaust mass flow is

$$\dot{m}_e = \rho AU$$

or in terms of the Mach number

$$\dot{m}_e = \left(\frac{PEH+\mathbf{B}}{RT_e}\right)\left(\frac{\pi D_e^2}{4}\right) M (g_c k RT_e)^{0.5} .$$

The Mach number is then

$$M = \dot{m}_e \left(\frac{RT_e}{PEH+\mathbf{B}}\right)\left(\frac{4}{\pi D_e^2}\right)(g_c k RT_e)^{-0.5}$$

but

$$\dot{m}_e = \dot{m}_a + \dot{m}_f$$

and

$$M = (\dot{m}_a + \dot{m}_f)\left(\frac{RT_e}{PEH+\mathbf{B}}\right)\left(\frac{4}{\pi D_e{}^2}\right)(g_c kRT_e)^{-0.5}$$

or

$$M = \frac{3.927(\dot{m}_a + \dot{m}_f)\ (T_e)^{0.5}}{PEH + \mathbf{B}} \quad .$$

APPENDIX C

UNCERTAINTY ANALYSIS

A determination of the uncertainties in the entrance nozzle and fuel mass flow calibrations, the entrance nozzle discharge coefficient and the overall air to fuel ratio and Mach number was made using the method described by Kline and McClintock [16]. Data given in Tables XVI through XIX are considered representative for the calculations considered and are used to compute representative uncertainties.

For a single sample measurement the value of a specific variable should be given in the format

$$x = \bar{x} \pm \delta x$$

where $\bar{x}$ is the mean value of the variable and δx is the estimated uncertainty in x. Having described the uncertainties in the basic variables of a relationship, it is now necessary to determine how these uncertainties propagate into the result. Consider the relation where the result R is the product of a sequence of terms.

$$R = (x_1^a)(x_2^b)(x_3^c) .$$

A reasonable prediction of the uncertainty in the result R is obtained using the Second Order Equation suggested by Kline and McClintock [16].

$$\Delta R = \left[\left(\frac{\partial R}{\partial x_1}\,\delta x_1\right)^2 + \left(\frac{\partial R}{\partial x_2}\,\delta x_2\right)^2 + \left(\frac{\partial R}{\partial x_3}\,\delta x_3\right)^2\right]^{0.5} \qquad (a)$$

Evaluating the partial derivatives appearing in equation (a) and normalizing by diving through by R gives a simplified form of equation (a) which will be used in this analysis.

$$\frac{\Delta R}{R} = \left[\left(\frac{a\delta x_1}{x_1}\right)^2 + \left(\frac{b\delta x_2}{x_2}\right)^2 + \left(\frac{c\delta x_3}{x_3}\right)^2\right]^{0.5} \qquad (b)$$

Determination of the uncertainty in the entrance nozzle mass flow ($\dot{m}_a$) is facilitated by writing $\dot{m}_a$ as a product of a series of terms.

$$\dot{m}_a = 0.099702(C_d)(Y)(d)^2(F)(1-\beta^4)^{-0.5}(PVH)^{0.5}(\Delta PV)^{0.5} \cdot (R)^{-0.5}(T_V)^{-0.5} \qquad (c)$$

Constants such as R can be assumed to have very small uncertainties in comparison with the measured data and therefore will be neglected in this analysis. Applying equation (b) to equation (c) yields the following expression for the uncertainty in $\dot{m}_a$:

$$\frac{\delta \dot{m}_a}{\dot{m}_a} = \left[\left(\frac{(1)\delta C_d}{C_d}\right)^2 + \left(\frac{(1)\delta Y}{Y}\right)^2 + \left(\frac{(2)\delta d}{d}\right)^2 + \left(\frac{(1)\delta F}{F}\right)^2 + \left(\frac{(0.5)\delta(PVH+\beta)}{PVH}\right)^2 + \left(\frac{(0.5)\delta\Delta PV}{\Delta PV}\right)^2 + \left(\frac{(-0.5)\Delta T_V}{T_V}\right)^2\right]^{0.5}$$

Using the values of the variables and their respective uncertainties listed in Table XVI, the uncertainty in the entrance nozzle mass flow rate is estimated to be

$$\frac{\delta \dot{m}_a}{\dot{m}_a} = 0.0046 = 0.46\% .$$

By a similar process the following representative uncertainties were estimated:

$$\frac{\delta C_{DN}}{C_{DN}} = 0.0083 = 0.83\% ,$$

$$\frac{\delta \dot{m}_f}{\dot{m}_f} = 0.0102 = 1.02\% ,$$

$$\frac{\delta M}{M} = 0.0063 = 0.63\% ,$$

$$\frac{\delta AFR}{AFR} = 0.011 = 1.11\% .$$

VARIABLE	VALUE	UNCERTAINTY (δ)
PNH+B	34.26 in Hg	± 0.1 in Hg
ΔPN	7.00 in H_2O	± 0.1 in H_2O
C_d	0.9840	± 0.0002
T_N	157 °F	± 1 °F
F	1.0018	± 0.0002
PVH+B	32.11 in Hg	± 0.05 in Hg
Y	0.8212	± 0.001
PV	9.25 in Hg	± 0.05 in Hg
T_v	158 °F	± 1 °F
d	2.130 in	± 0.002 in

TABLE XVI. Variables with Corresponding Uncertainties for Air Mass Flow Calculations.

VARIABLE	VALUE	UNCERTAINTY (δ)
$\dot{m}_a$	1.112 lbm/sec	± 0.005 lbm/sec
PNH+B	34.26 in Hg	± 0.1 in Hg
ΔPN	7.00 in H_2O	± 0.1 in H_2O
T_N	157 °F	± 1 °F
d_N	4.080 in	± 0.005 in

TABLE XVII. Variables with Corresponding Uncertainties for Entrance Nozzle Discharge Coefficient Calculation

VARIABLE	VALUE	UNCERTAINTY (δ)
f	101.0 Hz	± 0.1 Hz
time	98.66 sec	± 0.2 sec
fuel weight	1.00 lb	± 0.01 lb

TABLE XVIII. Variables with Corresponding Uncertainties for Mass Flowmeter Calibration Calculations.

VARIABLE	VALUE	UNCERTAINTY (δ)
$\dot{m}_a$	1.262 lbm/sec	± 0.006 lbm/sec
$\dot{m}_f$	49.5 lbm/hr	± 0.05 lbm/hr
d_N	4.080 in	± 0.005 in
PNH+β	37.37 in Hg	± 0.05 in Hg
ΔPN	8.42 in H_2O	± 0.05 in H_2O
T_N	173.6 °F	± 0.2 °F
PEH+β	31.90 in Hg	± 0.02 in Hg
T_e	850 °F	± 3 °F
D_e	7.500 in	± 0.002 in

TABLE XIX. Variables with Corresponding Uncertainties for Mach Number and Air to Fuel Ratio Calculations

BIBLIOGRAPHY

1. Pucci, P.F., Simple Ejector Design Parameters, Ph.D. Thesis, Stanford University, September, 1954.

2. Ellin, C.R., Model Tests of Multiple Nozzle Exhaust Gas Eductor Systems for Gas Turbine Powered Ships, Engineers Thesis, Naval Postgraduate School, June, 1977.

3. Moss, C.M., Effects of Several Geometric Parameters on the Performance of a Multiple Nozzle Eductor System, MS Thesis, Naval Postgraduate School, September, 1977.

4. Harrell, J.P., Experimentally Determined Effects of Eductor Geometry on the Performance of Exhaust Gas Turbine Powered Ships, Engineers Thesis, Naval Postgraduate School, September, 1977.

5. Naval Sea Systems Command Drawing No. 205-4539624 Rev. B, Arrangement of Gas Turbine Exhaust Uptakes, DD-963 Class, October, 1972.

6. General Electric Co., LM2500 Marine Gas Turbine Performance Data, MID-3-2500-8, September 1973.

7. The Chemical Rubber Company, Handbook of Tables for Applied Engineering Science, CRC Press, 1976.

8. Keenan, J.H. and Kaye, J., Gas Tables, John Wiley and Sons, Inc., 1963.

9. Streeter, V.L. and Wylie, E.B., Fluid Mechanics, p. 343-348, McGraw-Hill Book Company, 1975.

10. Boeing Airplane Company, Boeing Model 502-2E Gas Turbine Engine, February, 1953.

11. Carrier Corporation, Operating Instructions for Carrier Model 18P352 Air Compressor, October, 1955.

12. Hudson, R.G., The Engineer's Manual, p. 172, John Wiley and Sons, Inc., January 1963.

13. American Society of Mechanical Engineers Interim Supplement 1-.5 on Instruments and Apparatus, Fluid Meters, p. 224-233, Sixth Edition, 1971.

14. Woodward, John B., Marine Gas Turbines, John Wiley and Sons, Inc., 1975.

15. American Society of Mechanical Engineers, ATC 19.5-4, p. 19, 1959.

16. Kline, S.J. and McClintock, F.A., "Describing Uncertainties in Single Sample Experiments," Mechanical Engineering, p. 3-8, January, 1953.

INITIAL DISTRIBUTION LIST

		No. Copies
1.	Defense Documentation Center Cameron Station Alexandria, Virginia 22314	2
2.	Library, Code 0142 Naval Postgraduate School Monterey, California 93940	2
3.	Department Chairman, Code 69 Department of Mechanical Engineering Naval Postgraduate School Monterey, California 93940	2
4.	Professor Paul F. Pucci (Code 69Pc) Department of Mechanical Engineering Naval Postgraduate School Monterey, California 93940	10
5.	LT Charles R. Ellin 13512 Westwind Drive Silver Spring, Maryland 20904	1
6.	Mr. Charles Miller NAVSEA Code 0331 Naval Ship Systems Command Washington, D. C. 20362	1
7.	Mr. Olin M. Pearcy NSRDC Code 2833 Naval Ship Research and Development Center Annapolis, Maryland 21402	1
8.	Mr. Mark Goldberg NSRDC Code 2833 Naval Ship Research and Development Center Annapolis, Maryland 21402	1
9.	Mr. Eugene P. Wienert Head, Combined Power and Gas Turbine Branch Naval Ship Engineering Center Philadelphia, Pennsylvania 19112	1
10.	Mr. Donald N. McCallum NAVSEC Code 6136 Naval Ship Engineering Center Washington, D. C. 20362	1

		No. Copies
11.	Lt. J.P. Harrell, JR., USN 2004 Cloverleaf Place Ardmore, Oklahoma 73401	1
12.	Lt. C. M. Moss 625 Midway Road Powder Springs, Georgia 30073	1
13.	LCDR P. D. Ross, JR., USN 673 Chestnut St. Waynesboro, Va. 22980	2

Thesis
R7764 Ross
c.1 Combustion gas generator for gas turbine exhaust systems modeling.

174004